BRNO UNIVERSITY OF TECHNOLOGY
VYSOKÉ UČENÍ TECHNICKÉ V BRNĚ

FACULTY OF ARCHITECTURE
FAKULTA ARCHITEKTURY

DEPARTMENT OF EXPERIMENTAL DESIGN
ÚSTAV EXPERIMENTÁLNÍ TVORBY

FORM FOLLOWS WIND ENERGY
FORMOVÁNÍ STAVBY VĚTRNOU ENERGIÍ

MASTER'S THESIS
DIPLOMOVÁ PRÁCE

AUTHOR — **Bc. Jakub Brahmi**
AUTOR PRÁCE

SUPERVISOR — **B.Arch. Martin Kaftan, MSc, Ph.D.**
VEDOUCÍ PRÁCE

BRNO 2021

BRNO UNIVERSITY OF TECHNOLOGY
FACULTY OF ARCHITECTURE

Specification Master's Thesis

Project no.:	FA-DIP0015/2020
Department:	Department of experimental design
Student:	**Bc. Jakub Brahmi**
Study programme:	Architecture and urban design
Study field:	Architecture
Supervisor:	**B.Arch. Martin Kaftan, MSc, Ph.D.**
Academic year:	2020/21

Title of Master's Thesis:

Form follows wind energy

Master's Thesis:

This project is exploring possibilities of taking wind patterns as driving element for architectural design process in order to use and integrate the wind as one of the sources of energy in analogy to a way building volumes are often shaped for the benefit of gains. The Venturi effect is mostly taken as an undesirable phenomenon leading to discomfort due to higher wind speeds it is creating in urban areas. However, here it will be used in order to amplify the energy, so self–sufficient buildings can be possible to design even in places with relatively low winds. Consequently, this technology will affect the building's form, therefore, it requires to design also an appropriate structural solution to accommodate the form's flexibility.

Graphics scope :

1) Thesis
– intro
– hypothesis
– principles of sol–ution
– discussion
2) Graphics
– situation 1:500 – 1:2000
– drawing documentation of building 1:50 – 1:200
– construction details 3 x 1:10 – 1:25
– interior and exterior perspectives
– exploded axonometrics
– visualisation
3) Models
site model 1:500 – 1:2000
building model 1:50 – 1:200

List of literature:

Cody B., Forms Follows Energy: Using Natural Forces to Maximize Performance

Carpo L., Particlised: Computational Discretism, or The Rise of the Digital Discrete

Horden R., Light Architecture

Date of project specification Master's Thesis: 15.2.2021
the deadline for submission for the Master's Thesis: 24.5.2021

Master's Thesis is submitted in the scope determined by the project supervisor; in addition, one B1 exhibition panel and Master's Thesis in electronic form are submitted.

Bc. Jakub Brahmi student	B.Arch. Martin Kaftan, MSc, Ph.D. project supervisor	B.Arch. Martin Kaftan, MSc, Ph.D. head of the institute

Ing.arch. MArch Jan Kristek, Ph.D.
Dean

In Brno dated 15.2.2021

Prohlašuji, že jsem vypracoval tuto práci samostatně, pod vedením svého vedoucího za použití literatury uvedené na konci díla.

windcatcher

wind energy driven design

Jakub Brahmi
Diploma thesis 2020/2021
Form follows wind energy
Formování stavby větrnou energií
supervisor: B.Arch. Martin Kaftan, MSc, Ph.D.

Abstract

This project explores possibilities of taking wind patterns as a driving element for architectural form finding process in order to use and integrate the wind as one of the sources of energy. Integrated wind turbines have been used in several architecture projects, however, rather as an addition to high-rise buildings with the obvious advantage of reaching heights with faster airflows. The aim is to enable collection of wind energy in smaller scales where the potential is rather subtle and allows for wider and more conscious application in places where it otherwise wouldn´t be possible.
The starting point for extending the use of wind energy to other areas is the Venturi effect, whose occurrence in urban environment is mostly taken as an undesirable phenomenon leading to discomfort due to higher wind speeds that is creating in certain areas.
On the contrary, when predicted it is possible to benefit from it as with the increased wind speed the potential energy gains rise exponentially, thus lower height is required for collecting energy.

Abstract / *CZ*

Abstrakt

Diplomová práce zkoumá možnost využití větrného proudění jako hnacího elementu architektonického návrhu za účelem integrace větru jako jeden ze zdrojů získávání energie. Větrné turbíny byly již využity v několika architektonických projektech, spíše však jako doplněk k výškovým budovám, jejichž výška je zřejmým předpokladem pro snažší získávání větrné energie díky dosahu k rychlejším proudům vzduchu.
Tento projekt prověřuje skrze architektonický návrh možnost získávání energie z větru i v menších výškách, kde není energetický potenciál tak zřejmý, kvůli výrazně menším rychlostem větru.

Výchozím bodem pro rozšíření využití větrné energie je Venturiho efekt, jehož výskyt je možné pozorovat v urbánním prostředí především jako negativní jev působící nepohodlí obyvatelům města, kvůli zvýšeným rychlostem větru. Naproti tomu, když je venturiho efekt předpokládán, může být využit pro zrychlení proudění vzduchu a následného sběru energie.

Za účelem podpoření Venturiho efektu pro sběr energie zkoumá projekt, jaký má tvarové uspořádání vliv na proudění vzduchu. Za pomoci simulací proudění tekutin(CFD) a na základě hodinových dat povětrnostních podmínek vybrané lokality, odvozuje možné množství získané energie, různými tvarovými uspořádáními. Energetické zisky jsou srovnávány s předpokládanou energetickou náročností stavby a následně je skrze architektonickou studii prověřována využitelnost stavby jako vítr urychlujícího tvaru stejně tak, jako objektu umožňujícího běžné obývání.

1. Wind energy and its potential

Introduction

In a situation of climate crisis and ever-growing focus on renewable sources of energy with actions such as European Union´s Green Deal aiming at climate neutrality by 2050 (In focus: Renewable energy in Europe, 2020) is wind among other energy sources receiving more attention.

Despite wind energy production being very clean, as greenhouse gas emissions caused by manufacturing and construction of wind turbines are the lowest compared to other energy sources (Letcher, 2017), large-scale wind energy production comes with significant environmental risks.
Besides commonly observed disadvantages like planting large-scale wind turbines causing perception of deterioration of the landscape by the public (Molnarova et al., 2012), disturbance towards marine species in case of off-shore wind farms and endangerment of bats and birds on shore, noise pollution in proximity of settlements and danger of accidents by blades falling off (Letcher, 2017), large-scale wind turbines were found to have influence on climate and can lead to air temperature increase (Tummala et al., 2016) (Letcher, 2017).

Smaller and micro wind turbines can avoid these negative environmental aspects. As bringing wind energy collection closer to the built environment comes with other difficulties, identifying locations with small-scale wind energy collection potential requires special attention.

Wind energy in urban environment

Wind energy collection in urban settings comes with apparent difficulties compared to the use of wind turbines in large open spaces as buildings and trees act like obstacles and together with friction cause a large reduction in wind speed (Brown & DeKay, 2001). Because of turbulences in the flow caused by the buildings, the efficiency of wind turbines can be significantly lowered. However, there is not a lot of resources in relation to the nature of urban wind patterns and their dynamics (KC et al., 2019). There are various factors that have influence on the performance of mounted wind turbines, such as the shape of the roof the turbine is mounted on, wind direction, surrounding environment (Abohela et al., 2013) and urban morphology (Wang et al., 2017).
By the type of design, there are several variations of small wind turbines that are used in the urban environment.

1. Horizontal Axis Wind Turbines(HAWT) are similar to regular large-scale wind turbines, usually with fixed direction
2. Ducted Wind Turbines(DWT) are based on HAWTs which are equipped with an additional duct frame to increase their performance
3. Vertical Axis Wind Turbines(VAWT)

The difference in the axis of rotation results in different suitability for particular situations. Generally, HAWTs have better performance than VAWTs, however, they are able to capture wind in a single direction and turbulences in the flow result in lower efficiency. Compared to regular horizontal axis wind turbines the ducted ones can cope with turbulent flows better and capture more energy. Vertical axis wind turbines have lower efficiency than HAWT and DWT, on the other hand, they can work in all wind directions which can make them a more suitable solution in certain cases.

fig.1
Horizontal axis wind turbine

fig.2
Ducted wind turbine

fig.3
Vertical axis wind turbine

According to the way of application on the building wind turbines can be divided into three types:

1. Building Mounted Wind Turbines (BMWT) are installed as an additional element to an existing building volume
2. Building Integrated Wind Turbines (BIWT) are expected already as part the building's design

3. Building Augmented Wind Turbines (BAWT) are supported by the design of the building itself which by augmenting the flow of the wind is supposed to improve their performance (Arteaga-López et al., 2019).

In most cases wind turbines serve more as an addition to a building which works by itself, however, there are few cases where the design of a building incorporates wind turbines in a way that has influence on the design itself. One of the first buildings with integrated wind turbines is the Strata Tower. The BIWT produce 8% of the building's annual energy consumption.
Another building, the Bahrain World Trade Center (fig. 6), completed in 2008 and designed as two towers connected by bridges with three mounted large-scale horizontal axis wind turbines.
The turbines in combination with the building's design improving the air flow were supposed to cover 11-15% of the building's energy demand (Smith & Killa, 2007). Wind turbines of the constructed building appear to provide 8-10% of buildings energy demand.
However, the energy gains could have been higher, as a converging composition would perform better according to CFD analysis (Stathopoulos et al., 2018).
Later example of BAWT is found in Pearl River Tower (fig. 4), completed in 2011. It is equipped with large-scale vertical axis wind turbines placed in inlets located through the building volume which are predicted to increase speed of wind flowing through the building by a factor of 2.5 (Tomlinson et al., 2014).

fig.4
Pearl River Tower

fig.5
Strata Tower

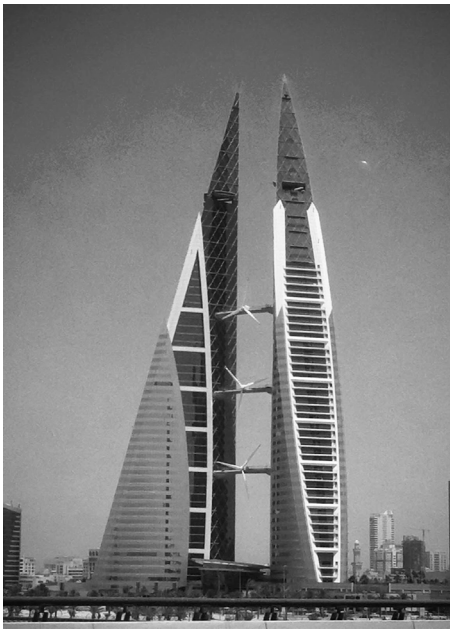

fig.6
Bahrain World Trade Center

Using venturi effect to increase wind energy collection

Venturi effect

The Venturi effect is a principle discovered by the Italian physicist Giovanni Battista Venturi who described relation of velocity and pressure of fluid flowing inside a conduit. When speed increases then pressure decreases and vice versa. If the conduit doesn´t have constant cross-section, velocity of the fluid increases according to the area of the cross-section (The Venturi effect. What it is and its application fields, n.d.). The lower the area of the cross-section the higher velocity and vice versa.

$$A_0 \cdot v_0 = A_1 \cdot v_1 = A_2 \cdot v_2$$

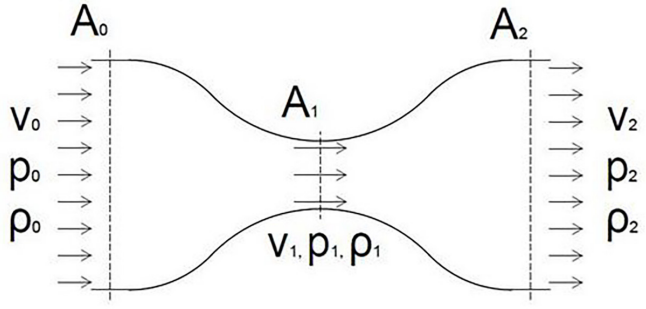

fig.7
Venturi effect (v - speed, A - area)
(source: https://www.pericoli.com/EN/news/119/The-Venturi-effect-What-it-is-and-its-application-fields.html)

Venturi effect in Architecture and Urbanism

The Venturi principle can be often observed as an undesirable effect in built environment in form of high wind speeds between buildings causing pedestrian discomfort, but architecture can also take advantage of it. In some cases, it can help to induce the natural ventilation (Cody, 2017) in order to save energy costs through avoiding HVAC. It can also be used to amplify energy collection in buildings with integrated wind turbines. The latter is to some extent used in the projects of Bahrain World Trade Center and Pearl River Tower.

Venturi effect as a design driver.

Previously mentioned buildings took advantage of the Venturi principle in relation to collection of wind energy. However, besides the effect itself these buildings have advantage of their height. The possible extent of use of Venturi principle through building's geometry even in smaller scales has been explored in this research.

Wind conditions in Europe

By collecting openly available data of mean wind speed in height 10m above ground and analyzing it through Geographic information system software it is possible to get overall image of potential locations for wind energy collection at the surface of the land.
In following graphic of Europe based on velocity values (fig. 8) it is obvious that higher wind speeds occur in areas of higher altitudes and coastal areas to the north-west and islands.
Because wind turbines have a certain cut in speed when they start collecting energy, they can´t be used in every case. Removing all areas with mean wind speed lower than required shows that not so many areas are suitable to collect wind energy right at the surface(fig.9).
In comparison after theoretical increase of wind speeds to 200% of original values wind energy potential would be accessible in much larger areas.

fig.8
Mean wind speed in Europe (in 10m)

fig.9
Areas with possible wind energy collection
(mean speed larger than 4m/s)

fig.10
Theoretical mean wind speed
increased to 200% (10m)

fig.11
Areas with possible wind energy collection
after theoretical speed increase (mean speed larger than 4m/s)

Specifying wind conditions at location from weather data files

To understand local wind conditions of a specific place it is necessary to analyze data in much higher-level detail. Airports and weather observation stations offer annual data of various weather conditions including measurements of wind directions and intensity. This data is often openly accessible and can be downloaded for free. Software such as Ladybug tools plugin for Rhino Grasshopper allows to convert this data to a wind rose graph which offers an overall picture of wind conditions at certain locations. Figure 12 demonstrates an example of wind rose graph created from wind data from Bergen airport in Norway.

fig.12
Wind rose of Bergen airport, Norway

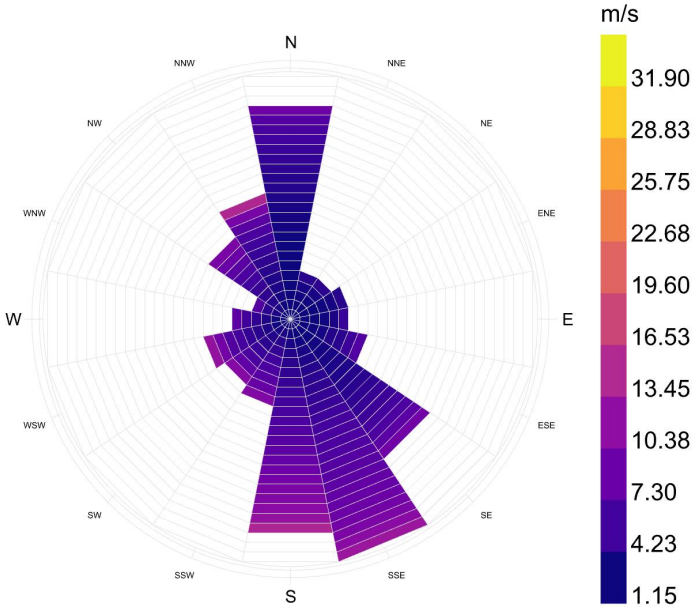

Estimating possible wind energy collection and building energy demand coverage

Previously mentioned weather data about wind speeds can be further decomposed as it bundles values for every single hour over the whole year. As wind turbines have certain lower and upper limits of wind intensity for functioning, values that aren´t in their domain have to be removed. With the remaining data it´s possible to estimate obtained annual energy.

$$P = \frac{1}{2} \cdot C_p \cdot \rho \cdot v^3 \cdot A$$

fig.13
Power (P) obtained by wind turbine
(Cp - power coefficient, ρ - air density(kg/m3), v - wind speed(m/s) , A - swept area of turbine(m2)

Using simple equation for power of wind turbine (fig. 13) derived from theoretical power of wind after including power coefficient of a wind turbine (Kosky et al., 2021) and applying it to hourly values gives a result of approximate annual energy gain in different directions. This resulting energy gain then when compared to determined annual building energy demand per square meter gives result of possible coverage of a building (figure 14).

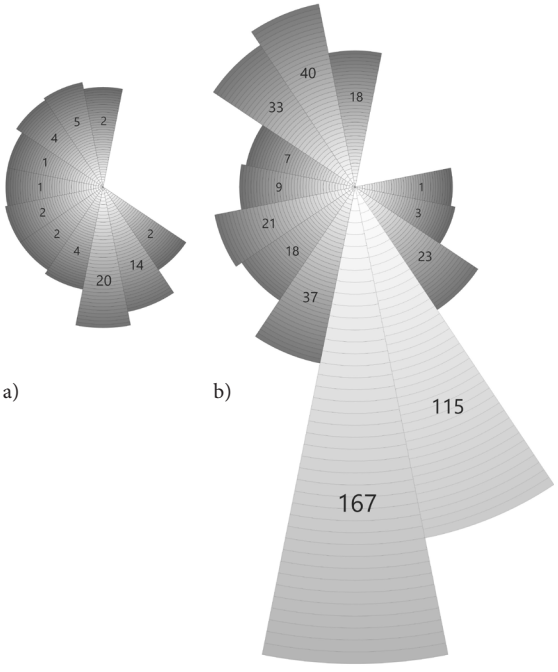

a) b)

fig. 14
Building area coverage potential based on data from Bergen airport
a)
building area(m2) energy coverage by a wind turbine (HAWT) from different directions under real conditions
- For building energy demand 15 kWh/m2
- Wind turbine diameter 1,5m

b)
building area(m2) energy coverage by a wind turbine (HAWT) from different directions after wind speed increase to 200%
- For building energy demand 15 kWh/m2
- Wind turbine diameter 1,5m

2. Funnel testing

Shape comparison
(based on simple funnel in 10x20x20m block)

To predict and evaluate wind patterns around objects CFD simulations(fig. 15) using software, such as OpenFoam in this case, is necessary.
Such simulations allow observation of wind flow passing from larger area to smaller and obtaining idea of principles for later shaped objects. Variations of different shapes such as smooth and polygonal, simple funnels and funnels with obstacles, funnels with multiple passages and funnels of different external shape were tested.
The speed inside the narrow vent was measured and compared with input speed to get the increase of original value.
Every model was tested with an input speed of 6m/s.
To ensure that the results of a simulation would be applicable in further evaluation of energy performance in following part of form finding for a building volume, a single model was tested for varying input speeds to observe the difference in resulting speed increase(figure 16) Maximum difference was 1,7%. Therefore following simulations were performed only for one input speed and their results were taken for additional calculations of energy gains.

fig.15
Openfoam simulation result visualisation via Paraview

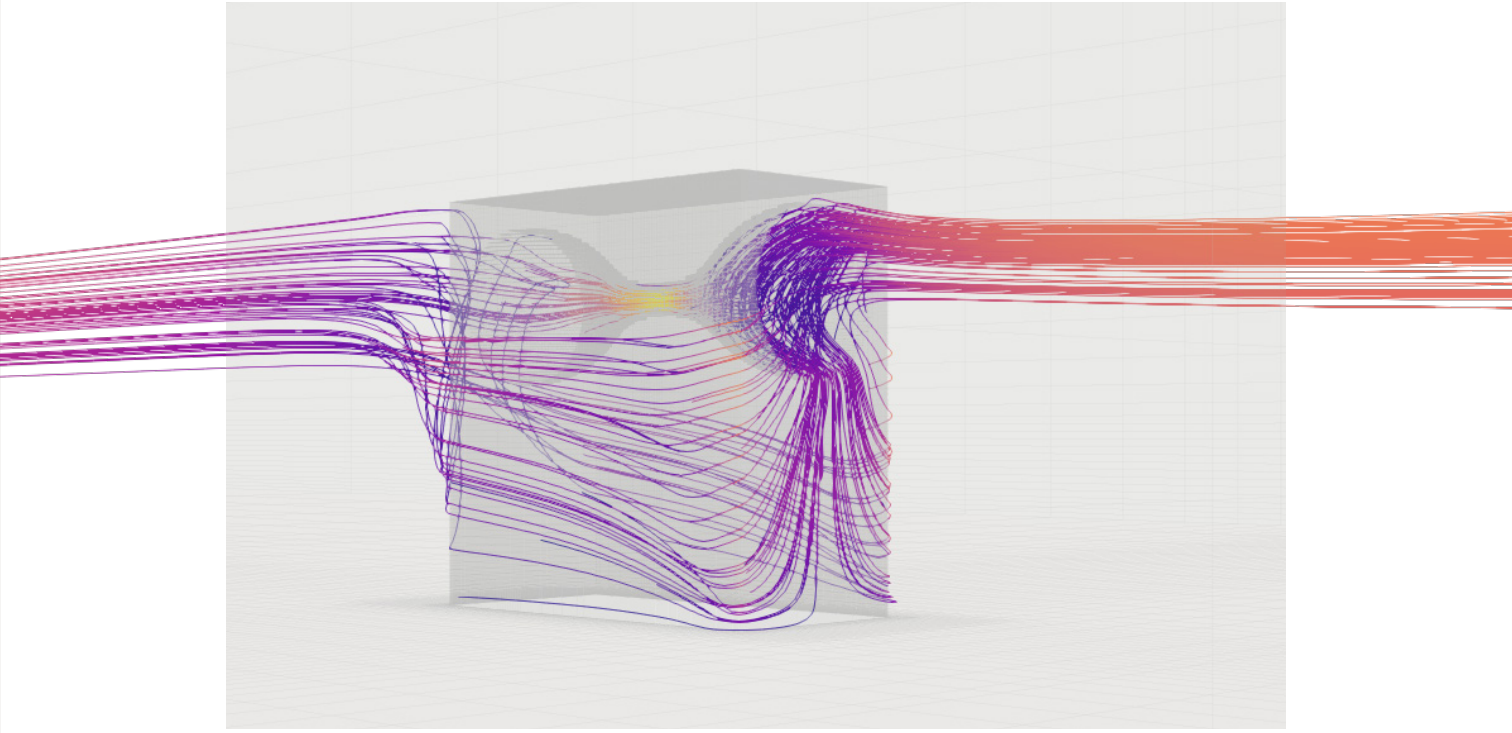

v1 (m/s)	v2 (m/s)	Increase (%)
2,00	3,53	176,5 %
4,00	7,07	176,8 %
6,00	10,62	177,0 %
8,00	14,17	177,1 %
10,00	17,72	177,2 %
12,00	21,26	177,2 %

fig.16
Difference in results depending on simulation input speed
(v1 - input speed, v2 - measured speed in the funnel)

Evaluation of these simple shapes with different funnels serves as a guidance for further design.
From results obtained it is obvious that in case of windflow in open space it is not possible to rely only on the ratio of area that is hit by the windflow and the area of narrower passage. As shown in figure 15, not all of the air flows through the passage and large part finds a way around the object. Generally smooth shapes performed better which might be obvious, however there are another more subtle notable aspects. As there is limited capacity to capture the flow in one passage adding more passages doesn´t result in lowered performance, it can even enhance the performance of each passage as seen in comparison of model 1.07 (fig. 17) and 1.13 (fig. 20). Differences not only inside the funnel influence the amount of air flowing through but also external shape of the whole volume as shown in model 1.07 (fig. 17) and models 1.26 and 1.27 (fig. 23) which all share the same internal funnel shape but differ in the shape of the whole volume.

fig.17
Funnel variants

model 1.01
speed increase: 144,9%

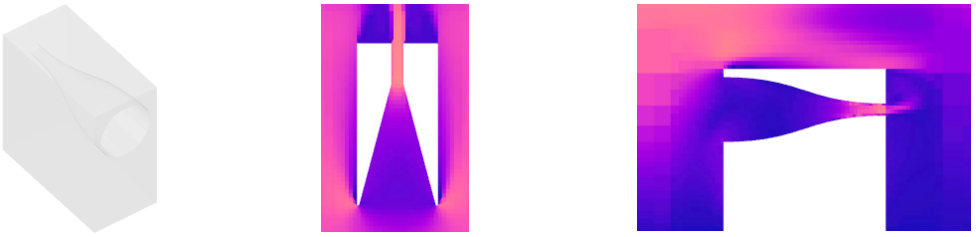

model 1.02
speed increase: 160,5%

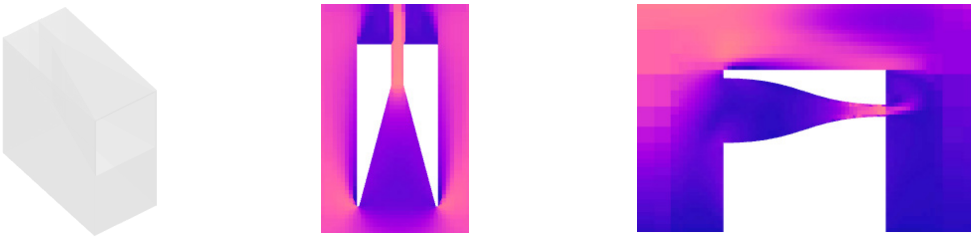

model 1.03
speed increase: 144,9%

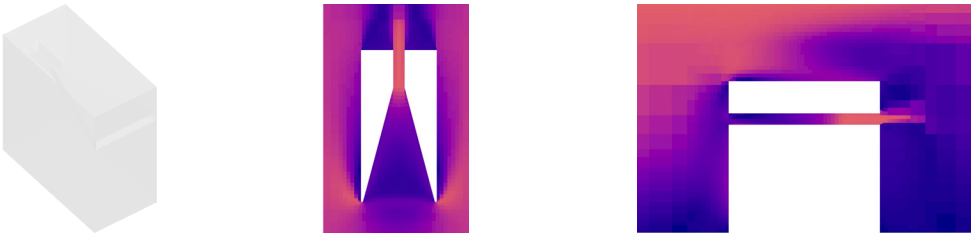

model 1.04
speed increase: 157,5%

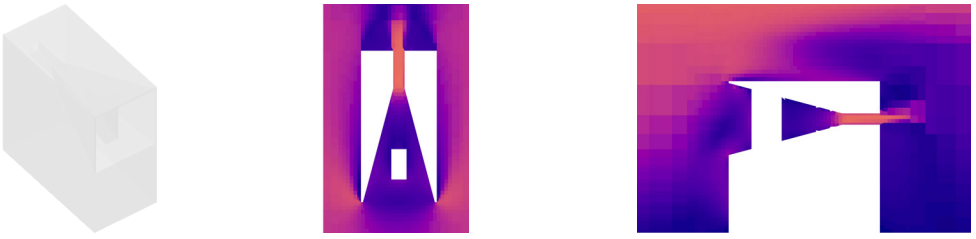

fig.18
Funnel variants

model 1.05
speed increase: 153,1%

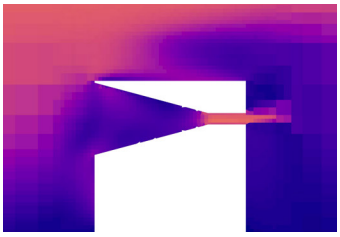

model 1.06
speed increase: 153,6%

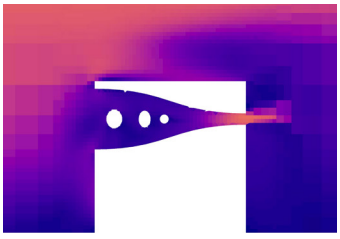

model 1.07
speed increase: 161,6%

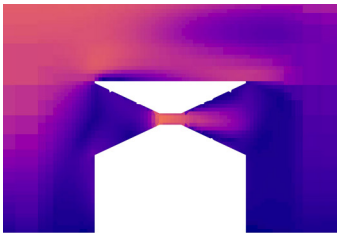

model 1.08
speed increase: 153,5%

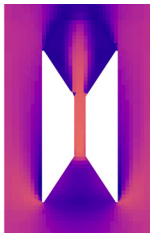

fig.19
Funnel variants

model 1.09
speed increase: 145,2%

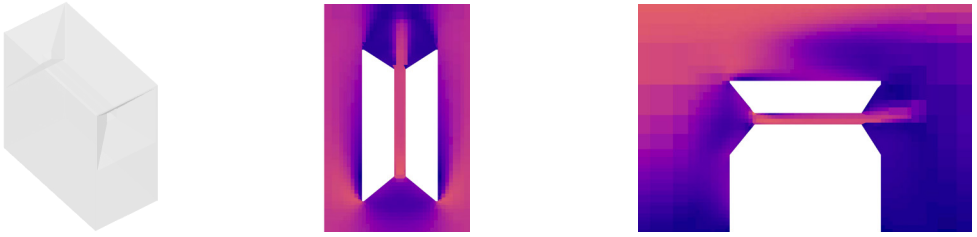

model 1.10
speed increase: 186,6%

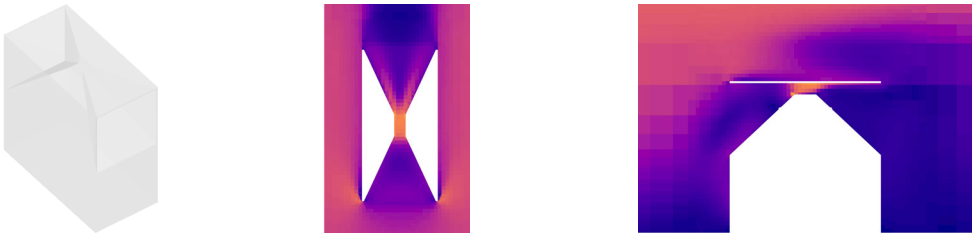

model 1.11
speed increase: 166,8%

model 1.12
speed increase: 174,7%

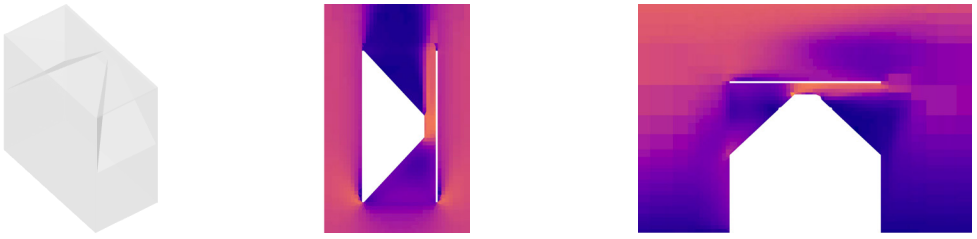

fig.20
Funnel variants

model 1.13
speed increase: 158,2%

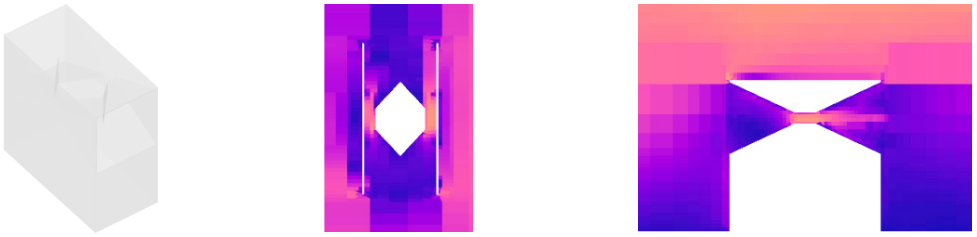

model 1.14
speed increase: 167,9%

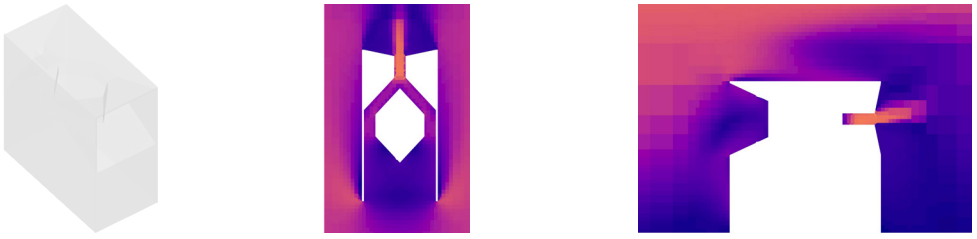

model 1.15
speed increase: 159,8%

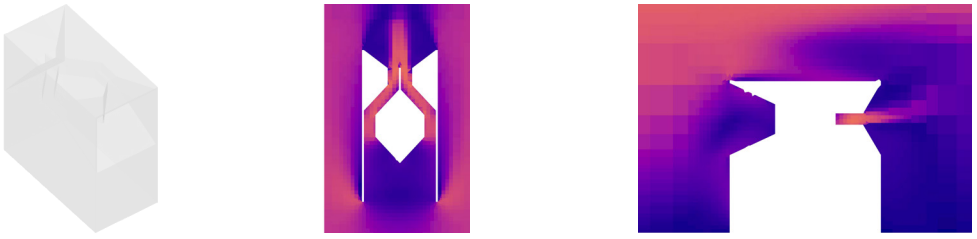

model 1.16
speed increase: 179,4%

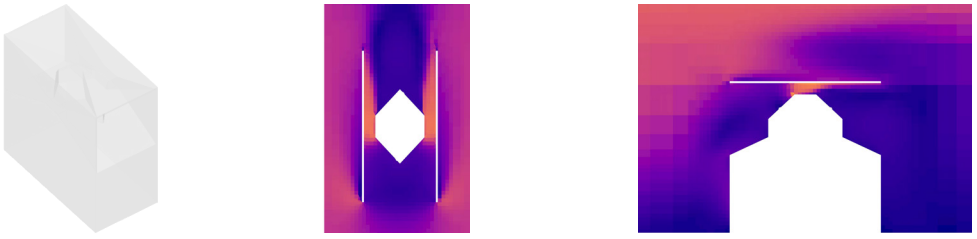

fig.21
Funnel variants

model 1.16
speed increase: 182,7%

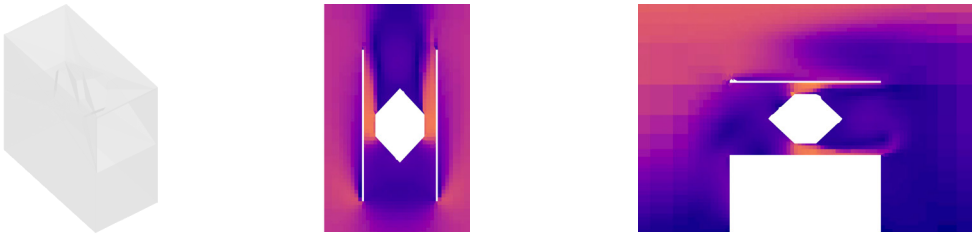

model 1.17
speed increase: 165%

model 1.18
speed increase: 189,3%

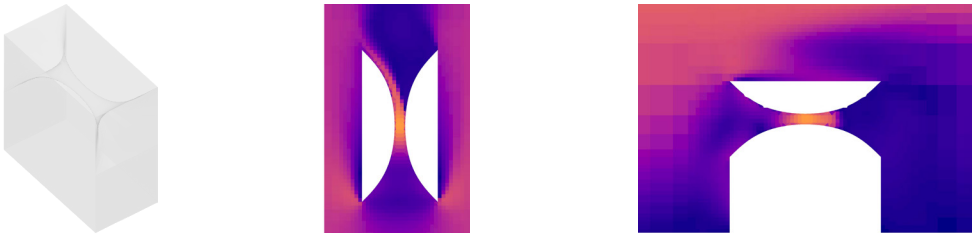

model 1.19
speed increase: 165,1%

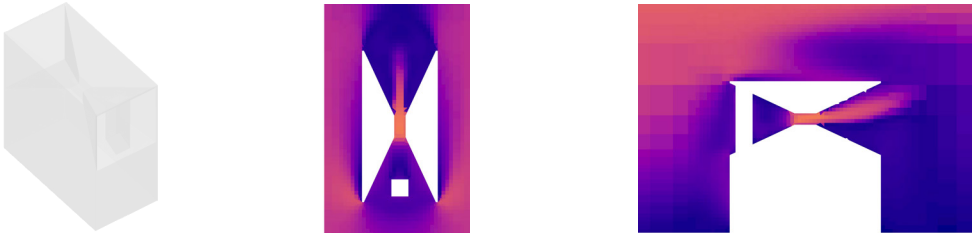

fig.22
Funnel variants

model 1.20
speed increase: 157%


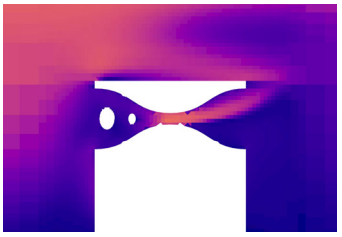

model 1.21
speed increase: 179,1%


model 1.22
speed increase: 140,8%


model 1.23
speed increase: 155,9%

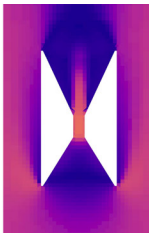
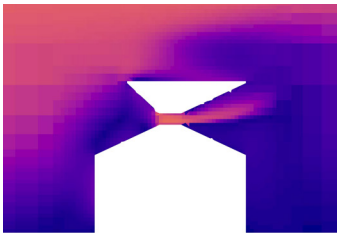

fig.23
Funnel variants

model 1.24
speed increase: 165,7%

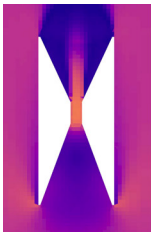

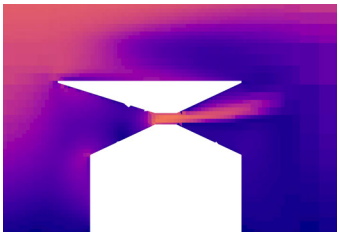

model 1.25
speed increase: 172,7%

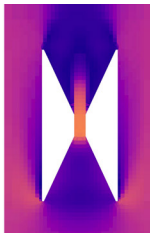

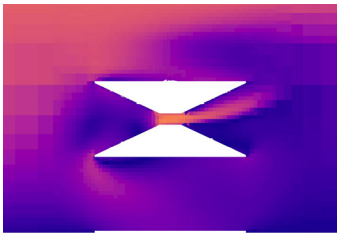

model 1.26
speed increase: 171,8%

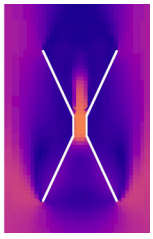

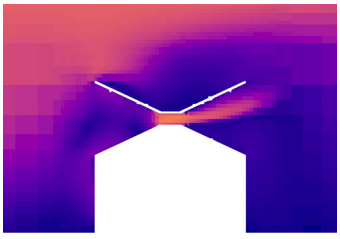

model 1.27
speed increase: 159,3%

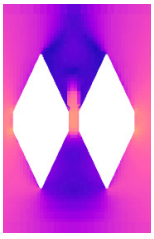

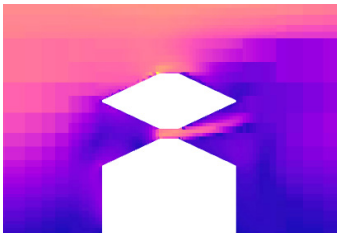

fig.24
Funnel variants

model 1.28
speed increase: 154,7%

model 1.29
speed increase: 177,3%

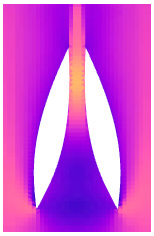

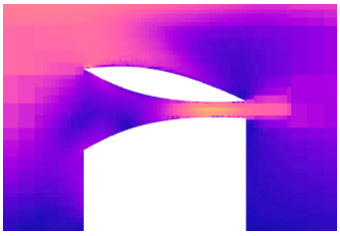

model 1.30
speed increase: 182,1

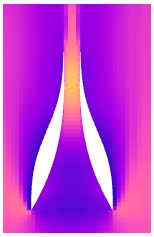

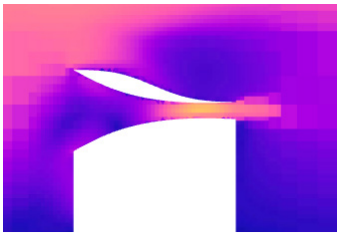

model 1.31
speed increase: 192,6%

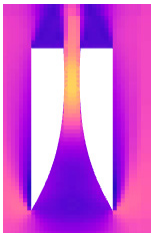

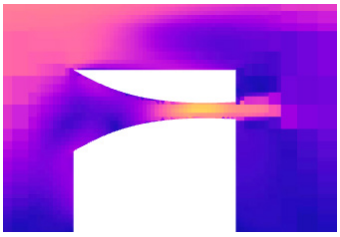

3. Case study - Form finding

Location

For the purpose of evaluation of applicability in architectural scale a location of Marignane near Marseille Airport (figure 27), based on available weather data, was chosen, particularly location on an empty field on the border of built area consisting of apartement buildings and detached houses. This location is characteristic with large concetration of winds in small range of angles (fig.25). No significant obstacles occur in the direction of prevailing wind.

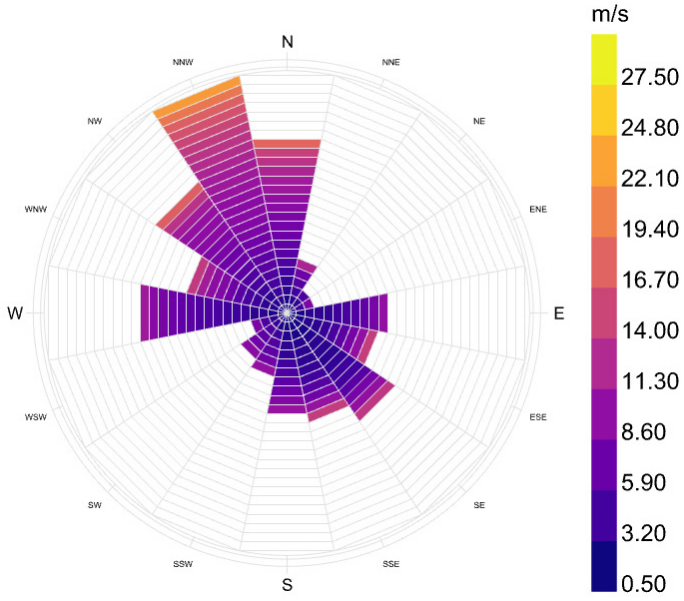

fig.25
Wind rose of Marseille airport, France

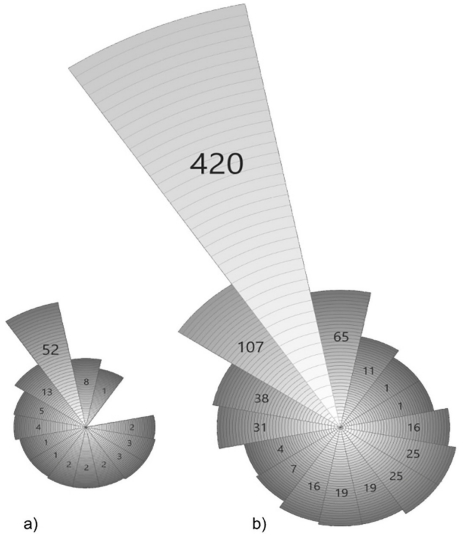

fig. 26
Building area coverage potential based on data from Bergen airport
a)building area(m2) energy coverage by a wind turbine (HAWT) from different directions under real conditions
- For building energy demand 15 kWh/m2
- Wind turbine diameter 1,5m

b) building area(m2) energy coverage by a wind turbine (HAWT) from different directions after wind speed increase to 200%
- For building energy demand 15 kWh/m2
- Wind turbine diameter 1,5m

fig.27
Location in Marignane and prevailing wind directions

Initial form

As a starting point a simple mass was created. Volume of the shape was kept in a scale of 6-storey apartment building to investigate energy collection potential in a small scale.
Shape of the volume was oriented towards the wind direction with the largest frequency of winds with high velocity, then split up into three separated parts to create a funneling area and smoothened following previous attempts where a smooth shape proved to be more effective.
These parts were then interconnected to enhance the funneling effect and created 4 passages through the volume at heights of 8 and 16 meters where wind turbines of a diameter 1,5m would be located (fig. 29), at each passage a single turbine.

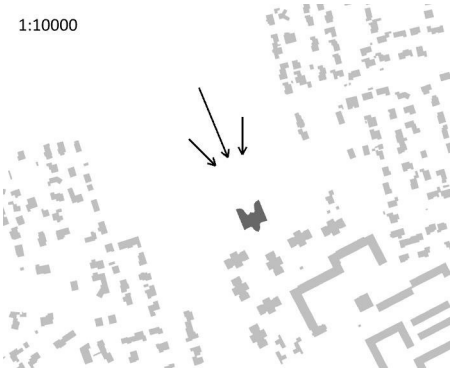

fig. 28
Location plan with prevailing wind directions and building volume

Several variations of rotation of volume parts on the sides in a converging, parallel and diverging shape (fig. 30) were then tested through CFD wind tunnel simulation using OpenFoam accessed through Butterfly for Grasshopper with input speed at a level of 10 meters above ground. At each of four passages through the building, a speed resulting from simulation of the main and secondary wind directions (fig.31) was measured and compared towards the input speed to obtain a ratio of acceleration.
After obtaining the acceleration ratio, hourly values of wind speed at the location were recalculated for each of the three directions to determine energy gains following the equation of power of a wind turbine (fig. 13).

fig.29
Composition scheme

fig.30
Tested variations of converging and diverging volumes

Evaluation of initial model

Of the five tested models, model 03 with a parallel configuration of connected volumes proved to be the most effective compared to the diverging and converging models. However, a more notable fact is that model 03 and model 04 performed in the secondary wind direction better than in the main wind direction that was used as an axis of symmetry for the building volume.

For this reason, model 03 was then tested again in three orientations (fig. 33), the original one and the variants rotated by 22.5 and 45 degrees to observe performance of the volume when its axis of symmetry is not facing the main wind direction.

There was not a significant difference in the performance of two rotated variants, with model rotated by 45° showing the best results (fig.32), however, both increased performance of the volume by approximately 30% compared to the model with original orientation.

The results show an uneven distribution of energy collection throughout the year. Larger energy collection occurs more often in autumn and winter months as shown in Figure 33.

A sum of the resulting energy gains was then compared to heating and cooling energy loads based on the approximated gross floor area of the volume if it was divided to 6 storeys and energy demand per square meter (passive standard (Passive House requirements, 2015) and average for Europe (Progress on energy efficiency in Europe, n.d.)).

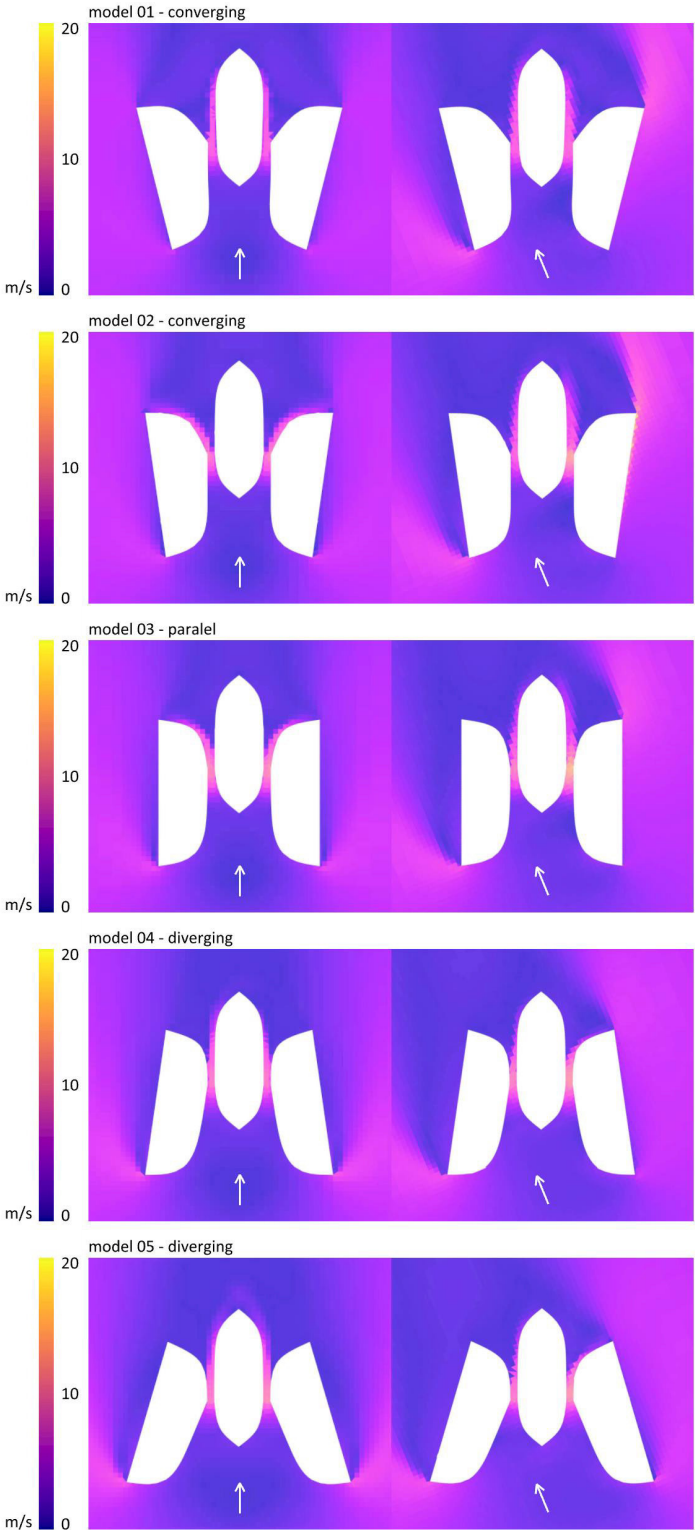

fig. 31
Simulation of variations of converging, parallel and diverging mass

In the case of average energy demand, the building model was able to capture only up to 4,1% of its own demand. However, in case of passive standard, the energy coverage was increased up to 41,7% of the building energy demand (fig.21).

Model 03	Acceleration for each turbine at different wind directions			Total energy production (kW)	Heating and cooling energy coverage	
Rotation	at 0°	at 315°	at 337,5°		Passive standart	Europe average (2016)
0°	224,3%	159,4%	175,4%	30444	31,0%	3,1%
	195,1%	154,3%	164,3%			
	158,1%	219,6%	179,2%			
	153,8%	195,8%	147,7%			
22,5°	227,3%	182,8%	227,8%	40643	41,4%	4,1%
	212,7%	174,6%	209,8%			
	209,8%	181,1%	161,1%			
	211,1%	176,2%	157,1%			
45°	119,5%	227,8%	228,5%	40928	41,7%	4,1%
	165,1%	211,0%	207,7%			
	112,0%	160,9%	209,8%			
	176,5%	157,4%	211,7%			

fig. 32
Model 03 evaluation – acceleration, energy gains, heating and cooling energy demand coverage

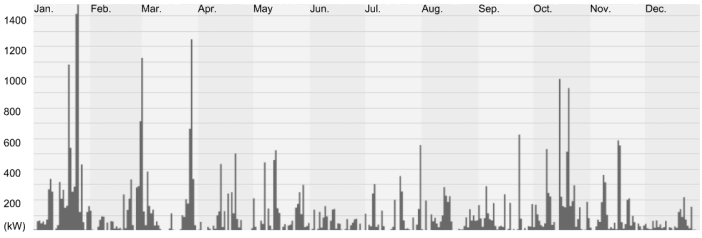

fig. 33
Energy collection throughout the year

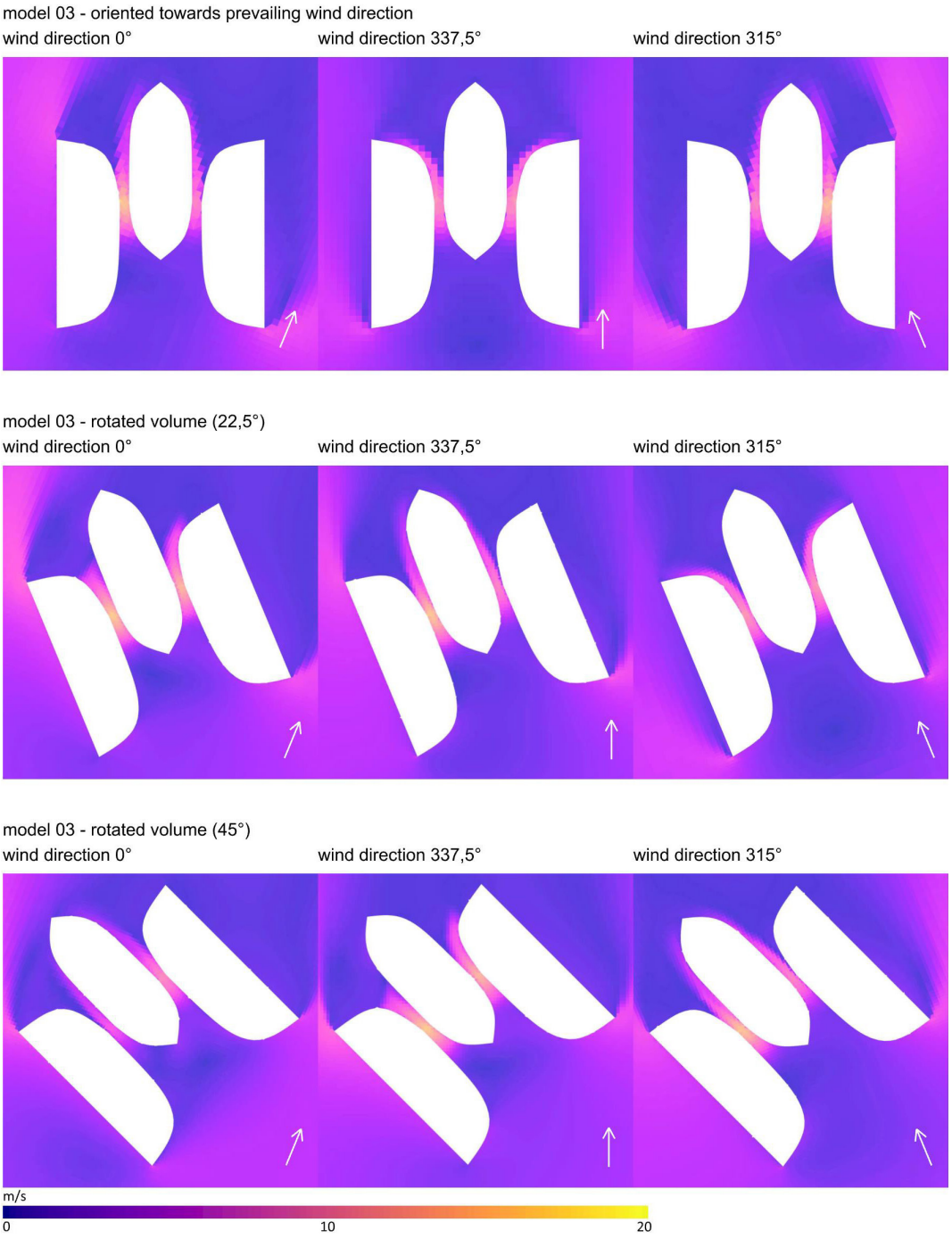

fig. 34
Simulation of variations of converging, parallel and diverging mass in varying orientation of the volume towards main wind direction

Subsequent transformations

As the goal is to design a building in scale of apartement building initial models would´n be sufficient for its use as the adjacent volumes create too enclosed space with insufficient access to direct sunlight.

Further shape explorations were therefore performed with various compositions both with larger and smaller differences in their shape through many iterations of shaping the volume. Various changes were made, such as lengthening and shortening of volumes, different orientations, smoothening and sharpening edges. Amount of vents was also changed through the adjustements.

To speed up evaluation of models, only the direction of prevailing wind was run through the CFD simulation and its results were then recalculated for potential anergy gain and compared to theoretical heating and cooling energy demand of passive standard building according to each models gross floor area.
Results of these evaluations are shown in figures 35-41. The obtained energy was calculated for windturbines of a diameter of 1,5m.

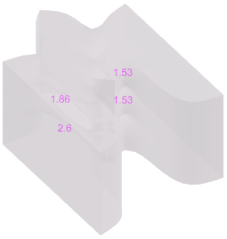

Model: 2.1
Energy Demand Coverage: 7.56 %

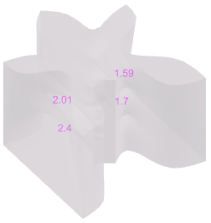

Model: 2.2
Energy Demand Coverage: 11.06 %

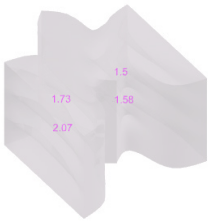

Model: 2.3
Energy Demand Coverage: 6.75 %

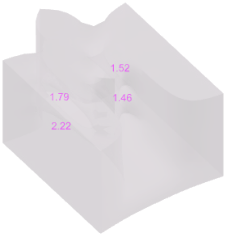

Model: 2.4
Energy Demand Coverage: 5.64 %

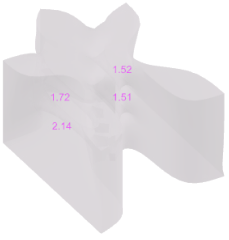

Model: 2.5
Energy Demand Coverage: 6.66 %

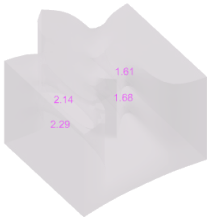

Model: 2.6
Energy Demand Coverage: 9.06 %

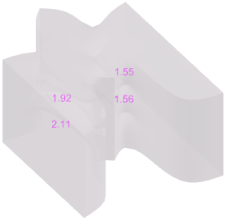

Model: 2.7
Energy Demand Coverage: 6.42 %

Model: 2.8
Energy Demand Coverage: 6.52 %

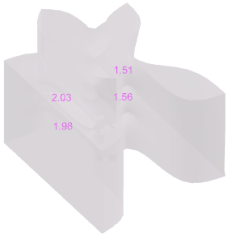

Model: 2.9
Energy Demand Coverage: 6.42 %

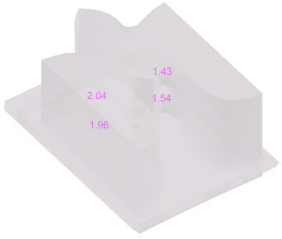

Model: 2.10
Energy Demand Coverage: 5.45 %

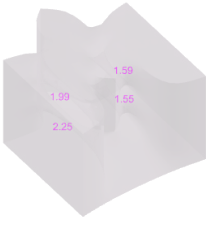

Model: 2.11
Energy Demand Coverage: 7.97 %

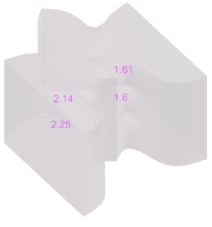

Model: 2.12
Energy Demand Coverage: 8.75 %

fig. 35 Volume transformations and performance

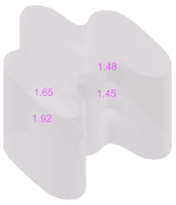

Model: 2.13
Energy Demand Coverage: 5.96 %

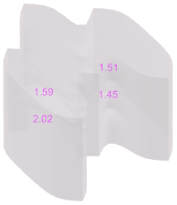

Model: 2.14
Energy Demand Coverage: 6.1 %

Model: 2.15
Energy Demand Coverage: 4.43 %

Model: 2.16
Energy Demand Coverage: 6.93 %

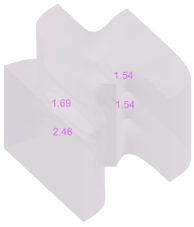

Model: 2.17
Energy Demand Coverage: 7.63 %

Model: 2.18
Energy Demand Coverage: 5.04 %

Model: 2.19
Energy Demand Coverage: 6.76 %

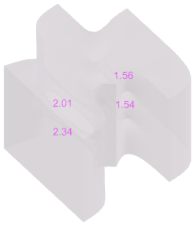

Model: 2.20
Energy Demand Coverage: 8.24 %

Model: 2.21
Energy Demand Coverage: 4.37 %

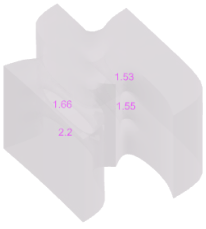

Model: 2.22
Energy Demand Coverage: 6.16 %

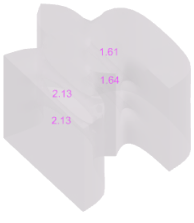

Model: 2.23
Energy Demand Coverage: 8.28 %

Model: 2.24
Energy Demand Coverage: 15.04 %

fig. 36 Volume transformations and performance

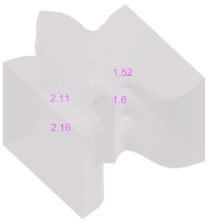

Model: 2.25
Energy Demand Coverage: 15.95 %

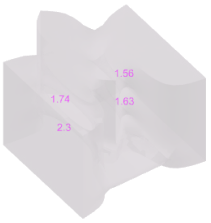

Model: 2.26
Energy Demand Coverage: 7.55 %

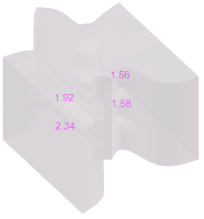

Model: 2.27
Energy Demand Coverage: 8.62 %

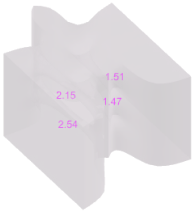

Model: 2.28
Energy Demand Coverage: 10.74 %

Model: 2.29
Energy Demand Coverage: 7.55 %

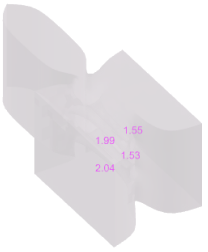

Model: 2.30
Energy Demand Coverage: 6.88 %

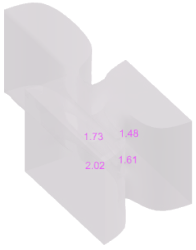

Model: 2.31
Energy Demand Coverage: 6.62 %

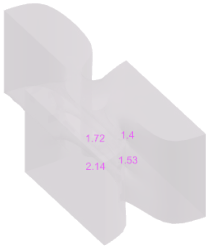

Model: 2.32
Energy Demand Coverage: 6.3 %

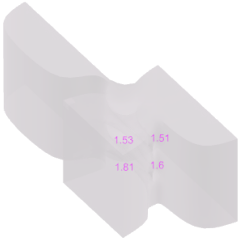

Model: 2.33
Energy Demand Coverage: 5.32 %

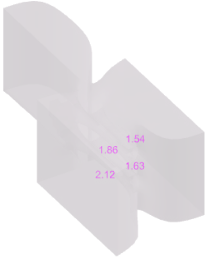

Model: 2.34
Energy Demand Coverage: 6.95 %

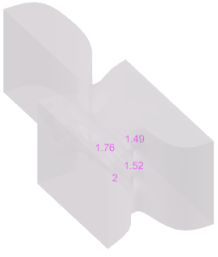

Model: 2.35
Energy Demand Coverage: 5.91 %

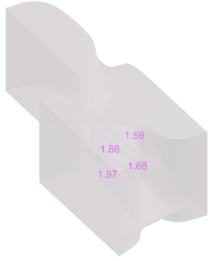

Model: 2.36
Energy Demand Coverage: 6.66 %

fig. 37 Volume transformations and performance

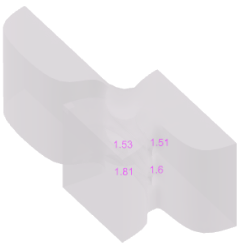

Model: 2.37
Energy Demand Coverage: 5.32 %

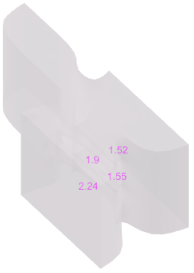

Model: 2.38
Energy Demand Coverage: 7.35 %

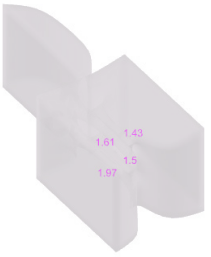

Model: 2.39
Energy Demand Coverage: 5.24 %

Model: 2.40
Energy Demand Coverage: 6.22 %

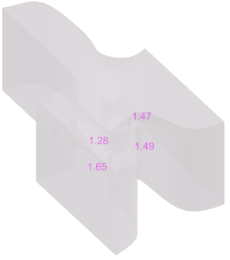

Model: 2.41
Energy Demand Coverage: 3.35 %

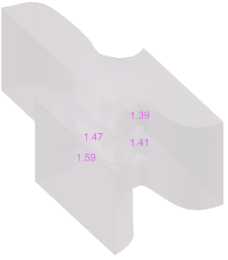

Model: 2.42
Energy Demand Coverage: 3.29 %

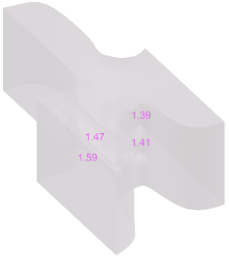

Model: 2.42
Energy Demand Coverage: 3.29 %

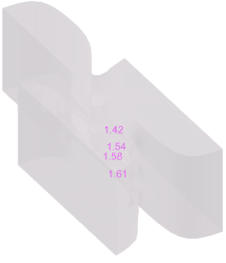

Model: 2.43
Energy Demand Coverage: 3.56 %

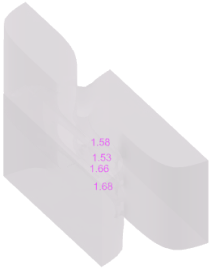

Model: 2.44
Energy Demand Coverage: 4.12 %

Model: 2.45
Energy Demand Coverage: 3.82 %

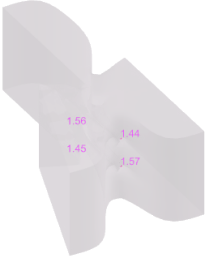

Model: 2.46
Energy Demand Coverage: 3.97 %

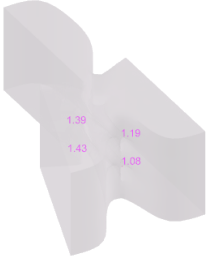

Model: 2.47
Energy Demand Coverage: 2.48 %

fig. 38 Volume transformations and performance

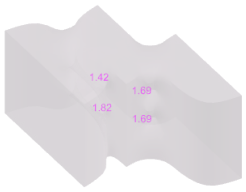

Model: 2.48
Energy Demand Coverage: 5.96 %

Model: 2.49
Energy Demand Coverage: 5.14 %

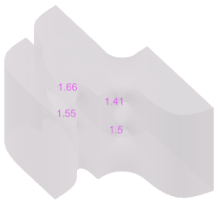

Model: 2.50
Energy Demand Coverage: 4.67 %

Model: 2.51
Energy Demand Coverage: 3.75 %

Model: 2.52
Energy Demand Coverage: 2.85 %

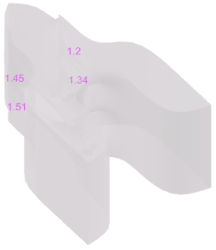

Model: 2.53
Energy Demand Coverage: 3.04 %

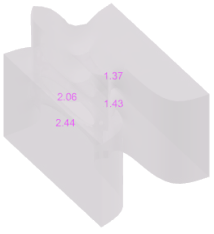

Model: 2.54
Energy Demand Coverage: 7.88 %

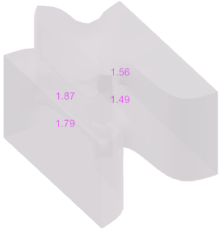

Model: 2.55
Energy Demand Coverage: 5.06 %

Model: 2.56
Energy Demand Coverage: 7.65 %

Model: 2.57
Energy Demand Coverage: 1.71 %

Model: 2.58
Energy Demand Coverage: 1.81 %

Model: 2.59
Energy Demand Coverage: 2.94 %

fig. 39 Volume transformations and performance

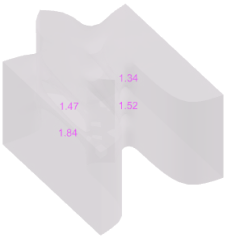

Model: 2.60
Energy Demand Coverage: 3.71 %

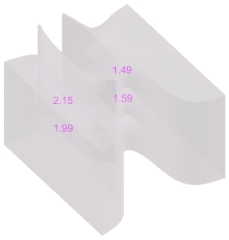

Model: 2.61
Energy Demand Coverage: 8.08 %

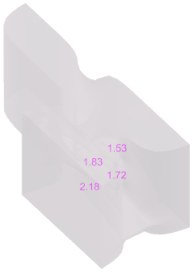

Model: 2.62
Energy Demand Coverage: 7.37 %

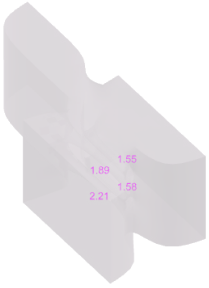

Model: 2.63
Energy Demand Coverage: 6.06 %

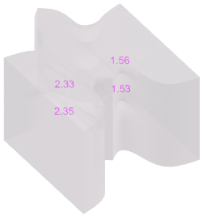

Model: 2.64
Energy Demand Coverage: 8.95 %

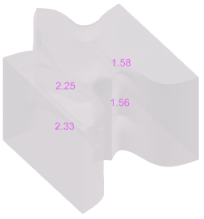

Model: 2.65
Energy Demand Coverage: 9.93 %

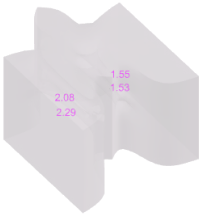

Model: 2.66
Energy Demand Coverage: 7.62 %

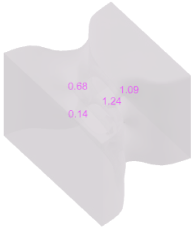

Model: 2.67
Energy Demand Coverage: 1.15 %

Model: 2.68
Energy Demand Coverage: 7.73 %

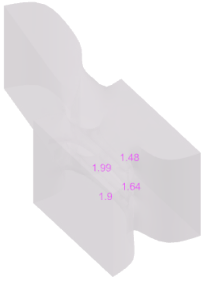

Model: 2.69
Energy Demand Coverage: 6.46 %

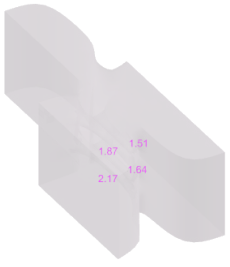

Model: 2.70
Energy Demand Coverage: 6.53 %

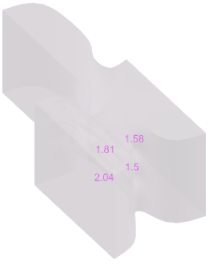

Model: 2.71
Energy Demand Coverage: 6.29 %

fig. 40 Volume transformations and performance

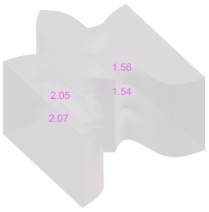

Model: 2.72
Energy Demand Coverage: 6.75 %

Model: 2.73
Energy Demand Coverage: 11.76 %

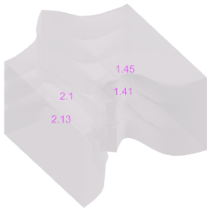

Model: 2.74
Energy Demand Coverage: 6.17 %

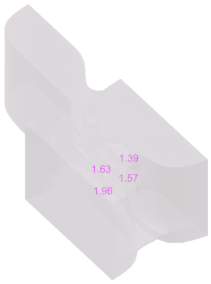

Model: 2.75
Energy Demand Coverage: 4.01 %

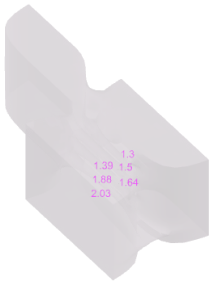

Model: 2.76
Energy Demand Coverage: 6.52 %

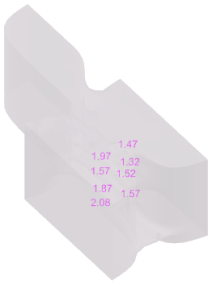

Model: 2.77
Energy Demand Coverage: 8.65 %

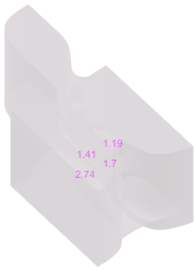

Model: 2.78
Energy Demand Coverage: 6.57 %

Model: 2.79
Energy Demand Coverage: 5.83 %

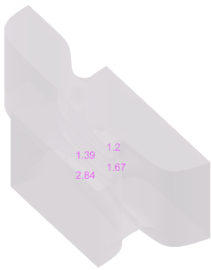

Model: 2.80
Energy Demand Coverage: 6.37 %

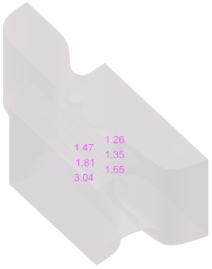

Model: 2.81
Energy Demand Coverage: 9.77 %

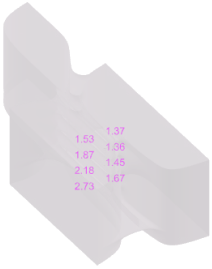

Model: 2.82
Energy Demand Coverage: 11.14 %

fig. 41 Volume transformations and performance

4. Case study - Design

Final shape

Final shape(fig.44), which is elaborated as an architectural study in following pages,is derived from model 2.81(figure 41), which was one of three models (2.80, 2.81, 2.82) of same shape with difference in number of vents. Same mass of volumes was kept but their distances from each other were adjusted to accomodate windturbines of larger diameter (2m) and slight changes to the shape of groundfloor were made.

Located in residential area near airport the building is designed as a mixed use building with larger part of residential use and offices in ground floor(fig.47). Most of the apartements(fig.46) consist of 2 rooms with exceptions of studio apartements. Corridors and communication cores are placed adjacent to the less lit area of the wind capturing enclosement and inhabited spaces are facing outwards from the whole volume.

The whole building is designed as three volumes constructed of CLT panels which are built on top of cast concrete base(fig.45). These volumes are enclosing external construction with wind speed enhancing effect where turbines are located as shown in construction scheme.

fig. 42
Schwarzplan 1:10000

fig. 43
Situation drawing 1:2000

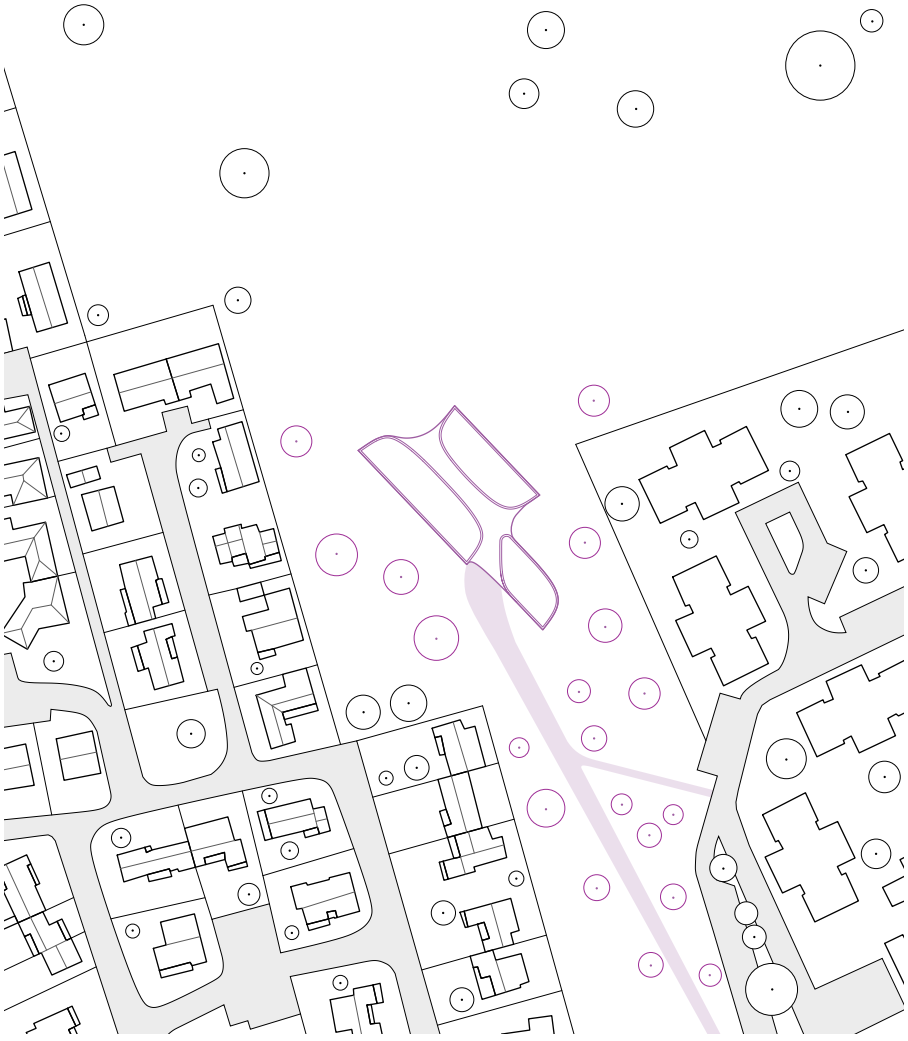

fig. 44
Axonometric views

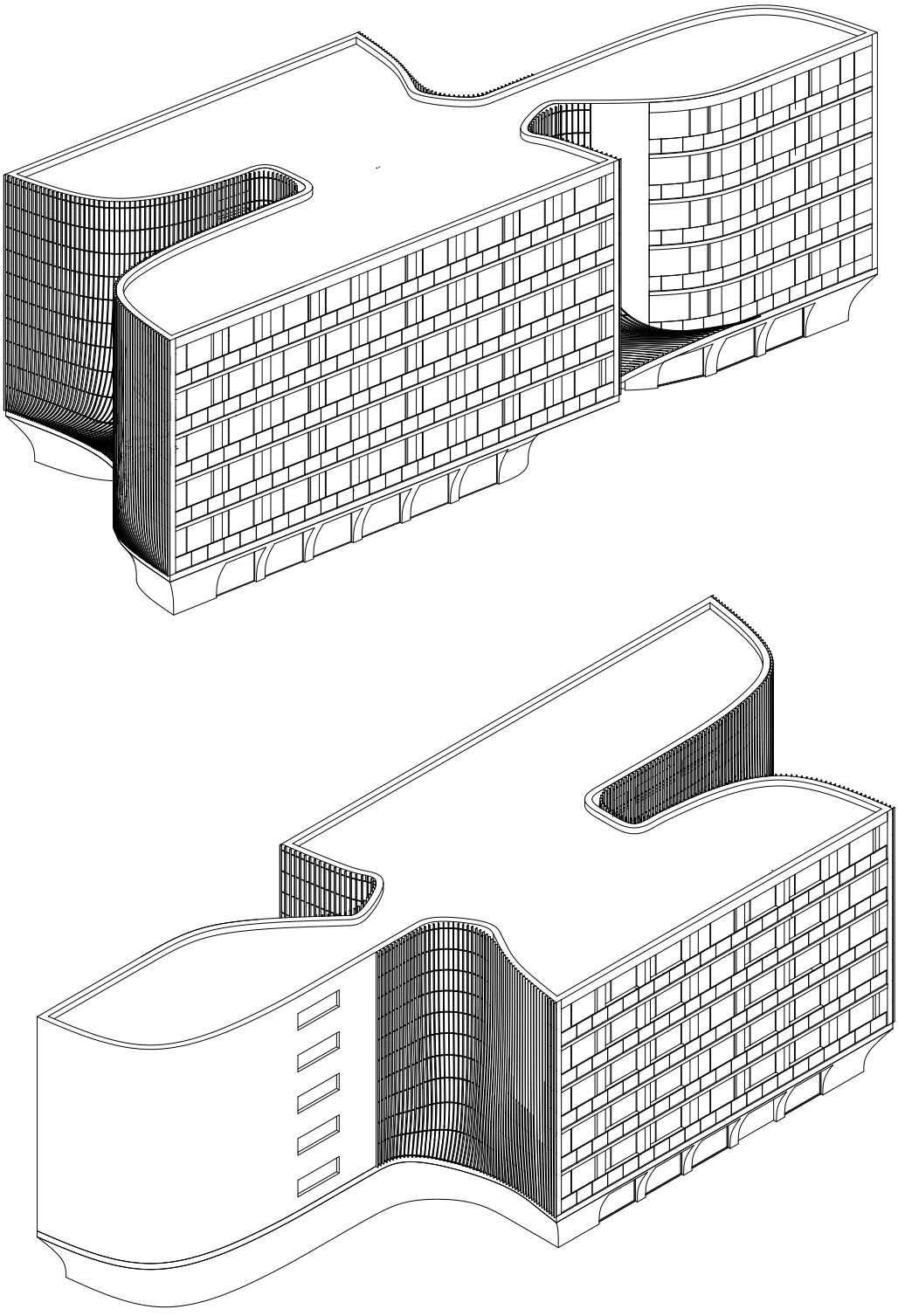

fig. 45
Construction scheme

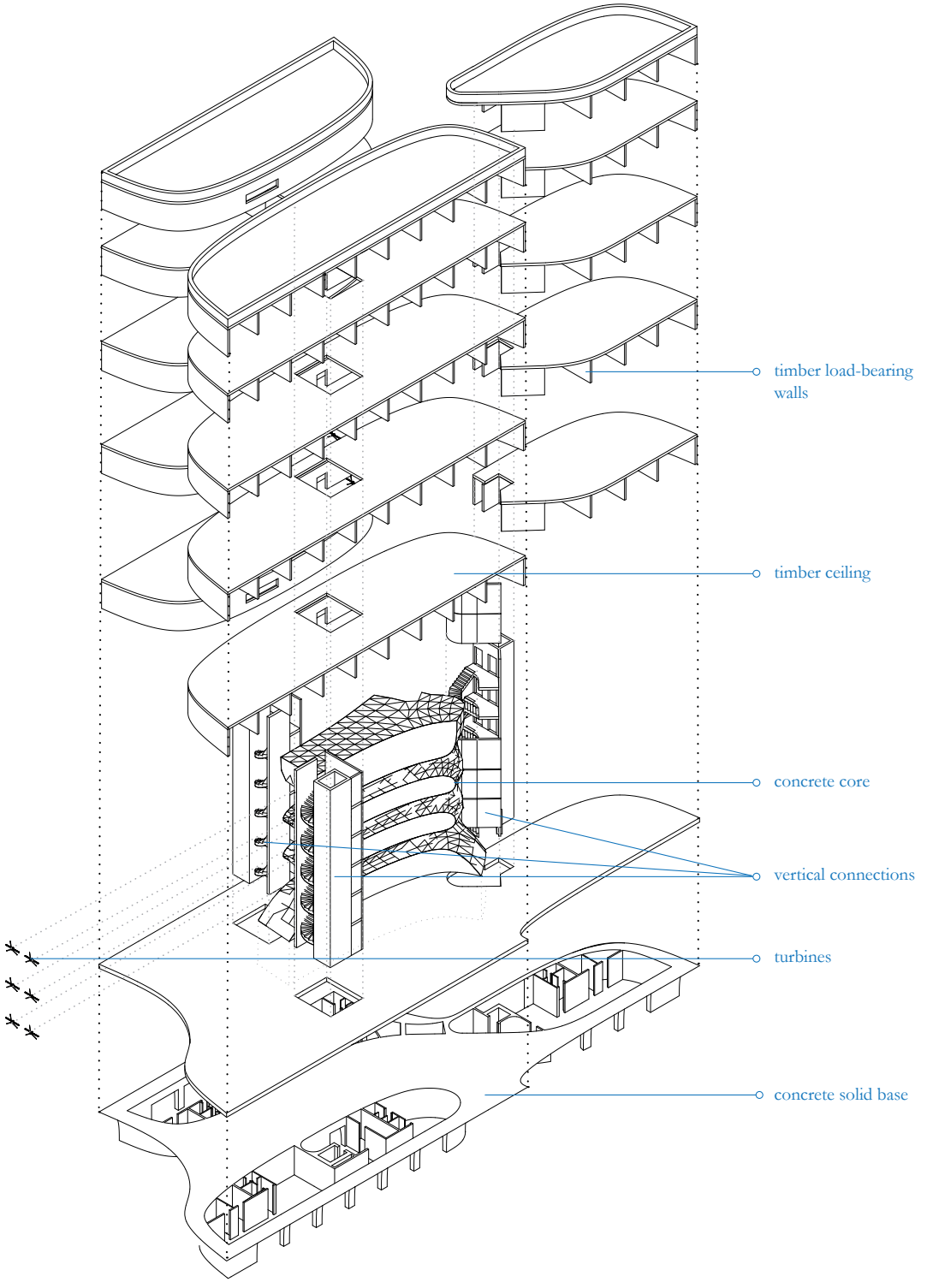

fig. 46
Groundplan of 2nd - 6th floor - residential

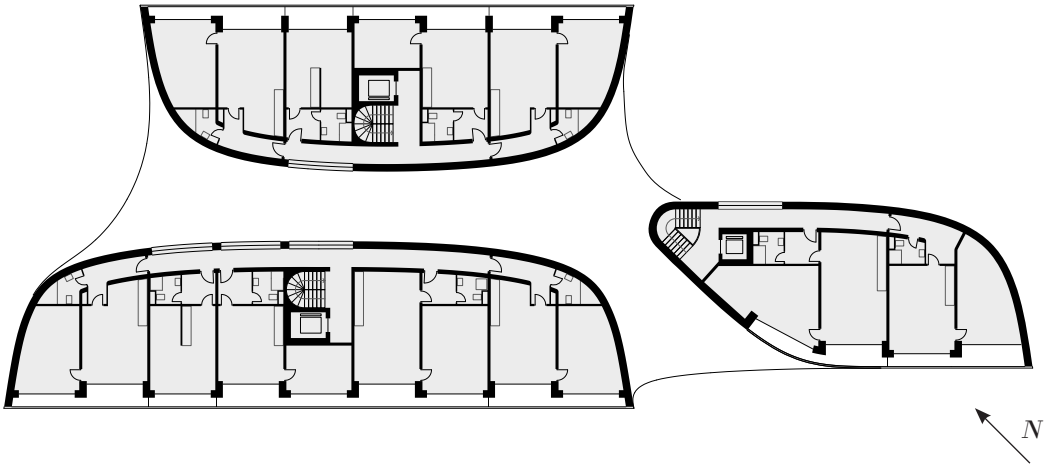

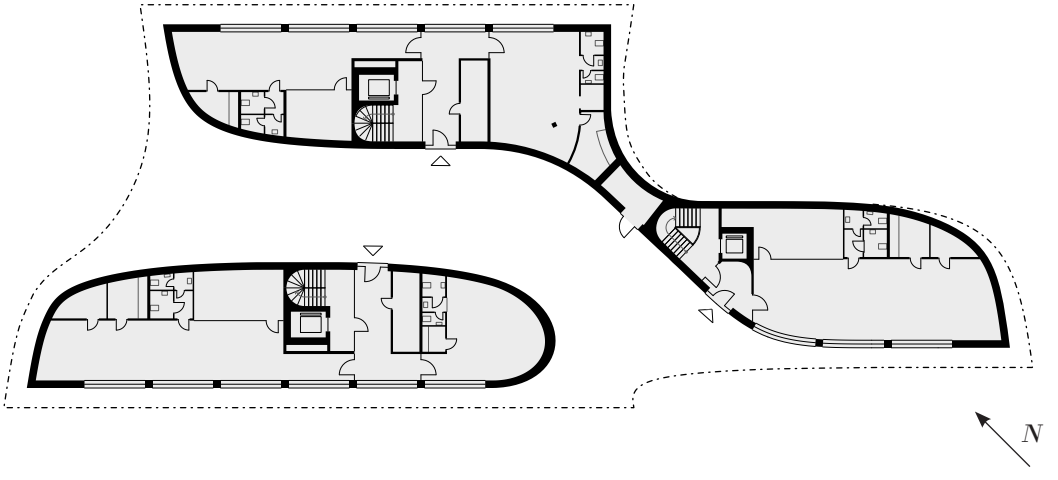

fig. 47
Groundplan of 1st floor - offices

10 5

fig. 48
Sections

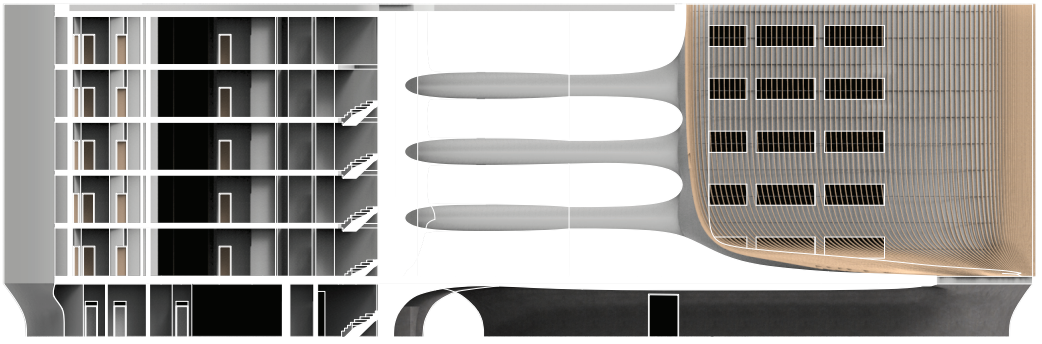

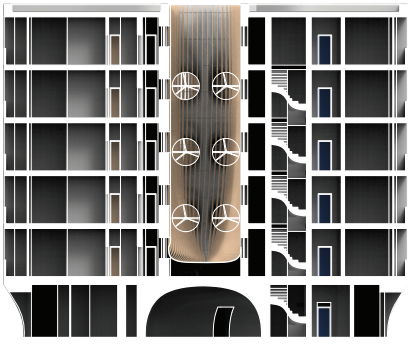

fig. 49
Elevations - south-west, north-east

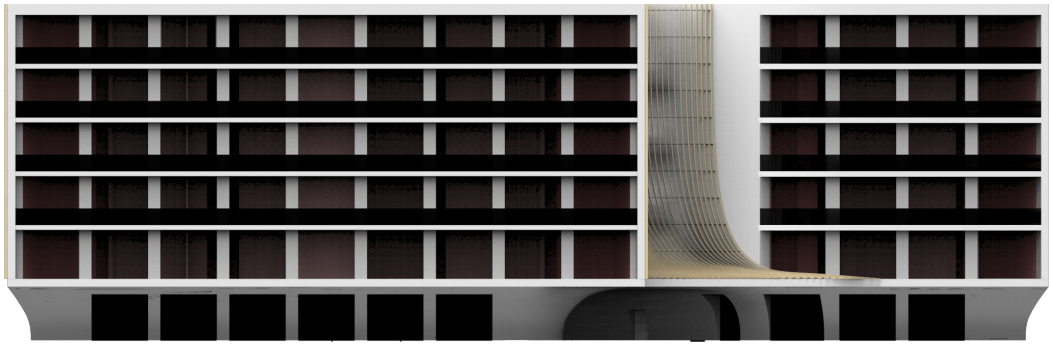

fig. 50
Elevations - north-west, south-east

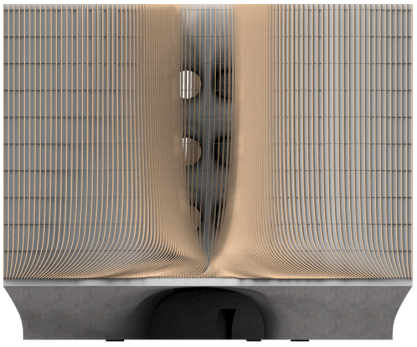

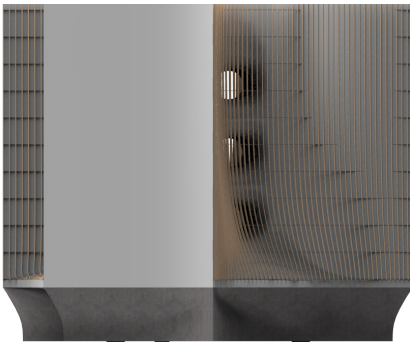

fig. 51
Detail 1:20
CLT (flat-flat) wall connection to concrete ceiling slab

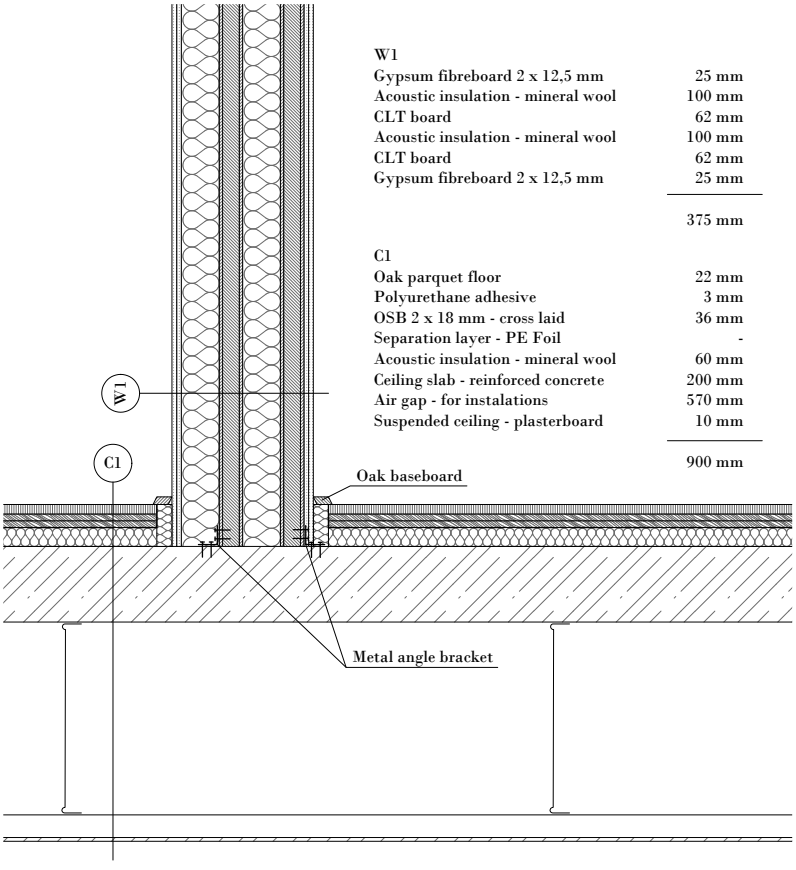

W1	
Gypsum fibreboard 2 x 12,5 mm	25 mm
Acoustic insulation - mineral wool	100 mm
CLT board	62 mm
Acoustic insulation - mineral wool	100 mm
CLT board	62 mm
Gypsum fibreboard 2 x 12,5 mm	25 mm
	375 mm

C1	
Oak parquet floor	22 mm
Polyurethane adhesive	3 mm
OSB 2 x 18 mm - cross laid	36 mm
Separation layer - PE Foil	-
Acoustic insulation - mineral wool	60 mm
Ceiling slab - reinforced concrete	200 mm
Air gap - for instalations	570 mm
Suspended ceiling - plasterboard	10 mm
	900 mm

fig. 52
Detail 1:20
CLT (flat-flat) wall connection to CLT (room-room) wall

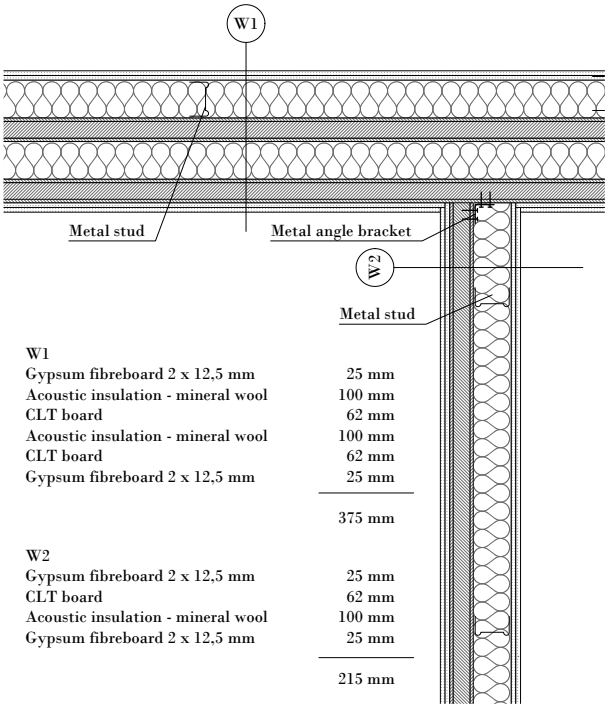

W1	
Gypsum fibreboard 2 x 12,5 mm	25 mm
Acoustic insulation - mineral wool	100 mm
CLT board	62 mm
Acoustic insulation - mineral wool	100 mm
CLT board	62 mm
Gypsum fibreboard 2 x 12,5 mm	25 mm
	375 mm

W2	
Gypsum fibreboard 2 x 12,5 mm	25 mm
CLT board	62 mm
Acoustic insulation - mineral wool	100 mm
Gypsum fibreboard 2 x 12,5 mm	25 mm
	215 mm

fig. 53
Detail 1:20
Exterior wall

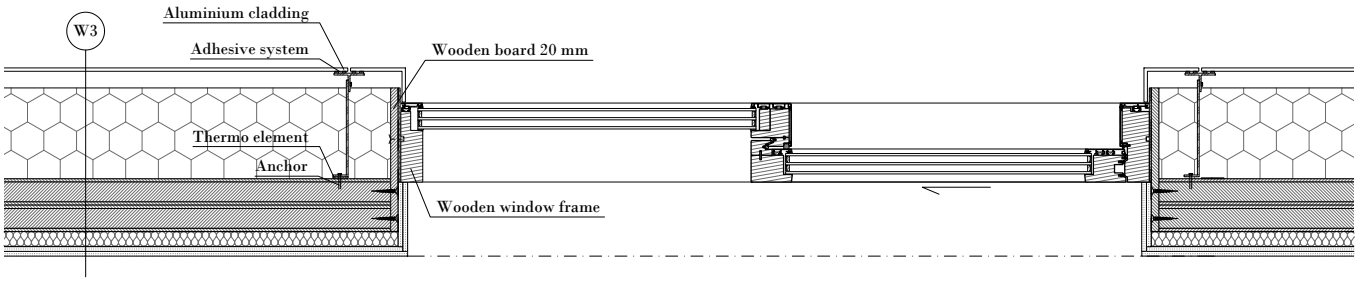

W3	
Gypsum fibreboard 2 x 12,5 mm	25 mm
Thermal insulation - mineral wool	37 mm
Vapor barrier	-
CLT board	140 mm
Thetmal insulation - EPS 0,031 W/(m2K)	240 mm
Gap	45 mm
Aluminium cladding	10 mm
	500 mm

fig. 54
Exterior perspective

fig. 55
Interior perspective
- groundfloor office

5. *Case study - Evaluation*

Additional evaluations for final model were performed as during design process mild changes to the dimensions of the volume were made in order to accomodate residential function into the building properly. Passages were increased to fit the 6 turbines of 2m diameter. These adjustements led to change in performance. Maximum increase(fig.56) in speed in main wind direction decreased compared to model 2.81 (fig.41) that served as template for further design. However, total energy gains were increased through larger swept area of turbines.

To evaluate overall performance of wind energy collection in the building, the total wind energy gains were set against estimated energy demands of the building based on energy demand simulation of the volume with set exterior wall composition (fig. 53). Additionally wind energy gains were compared to simulated solar energy potential for mounted PV panels.

In total wind energy provided for 41,9 percent of the annual buildings energy demands(fig. 59). At this location solar power produces more energy annualy. However in this case wind energy can serve as complementary source as calculations of daily values show that performance of both energy sources is changing throughout the seasons of the year(fig.60,61). While peak performance of solar power is in summer months, largest wind energy collection occurs in winter. An advantage of wind power compared to solar power is that it can also compensate for outage of solar energy production during night hours as a large part of its production occurs at night(fig.60).

Turbine	Increased speed at 0° (%)	Speed increase at 337,5°(%)	Speed increase at 315° (%)
1	174	147	146
2	196	206	161
3	182	150	153
4	196	201	160
5	199	162	169
6	214	201	173

fig. 56
Speed increase for each turbine

Energy demand	kWh/m2
Heating	6,76
Cooling	8,11
DHW	3,68
Lighting	8,24
Equipment	8,91
Electric fan	2,39
Total	38,09

fig. 57
Building energy demand per square meter

Annual energy demand	204822 kWh
Annual wind energy gains	85814 kWh
Annual PV energy gains	171672 kWh

fig. 58
Annual energy production and demand

Demand coverage	%
Wind energy	41,9
PV energy	83,8
Total	125,7

fig. 59
Energy coverage

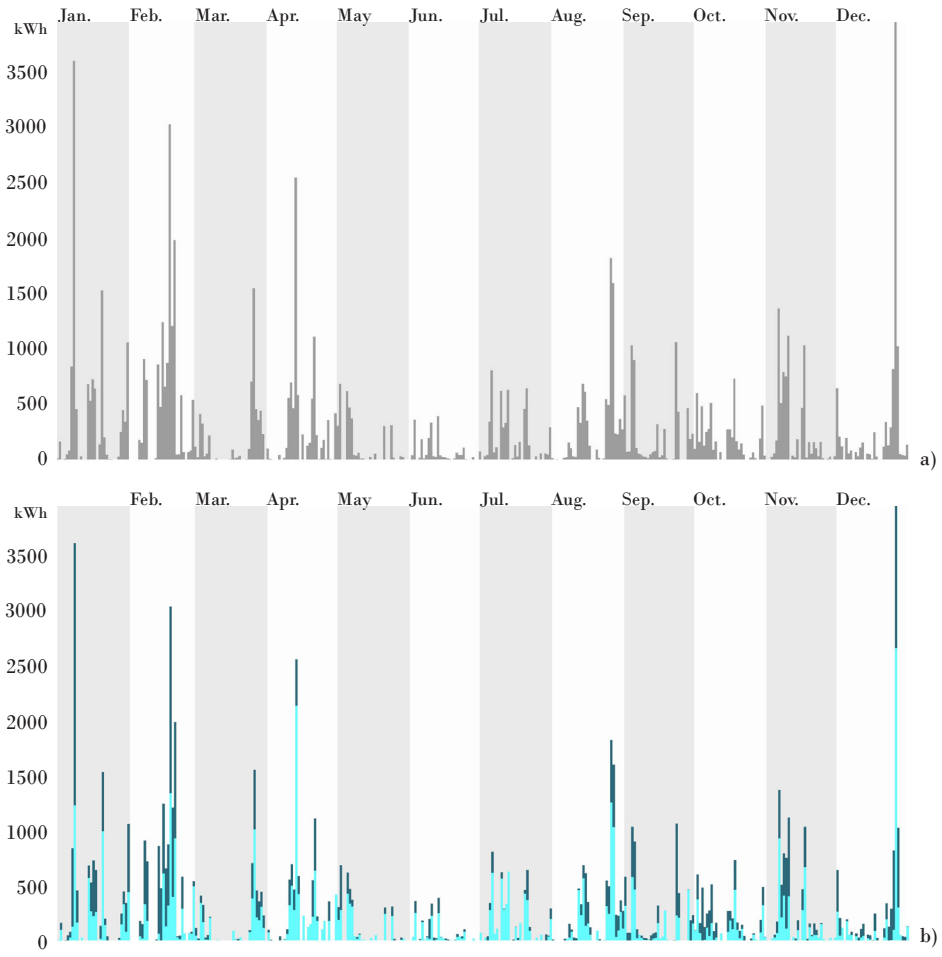

fig. 60
Wind energy gains throughout the year
a) total gains b) gains during day and night

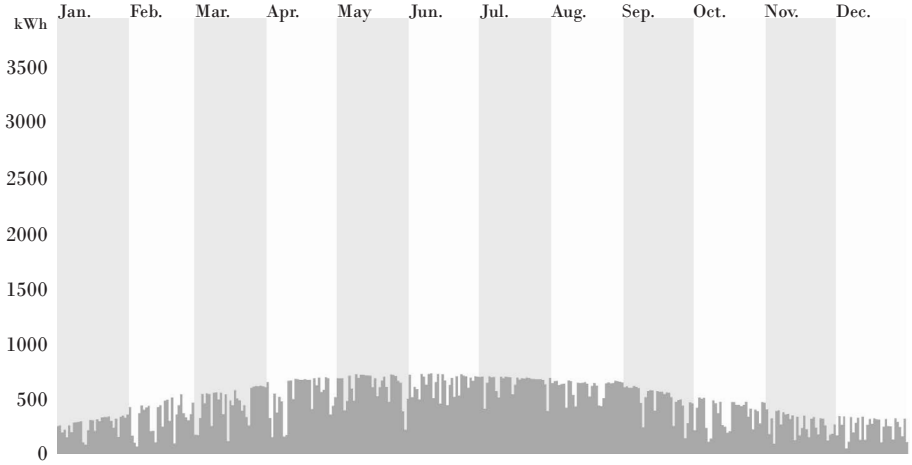

fig. 61
Solar energy gains throughout the year

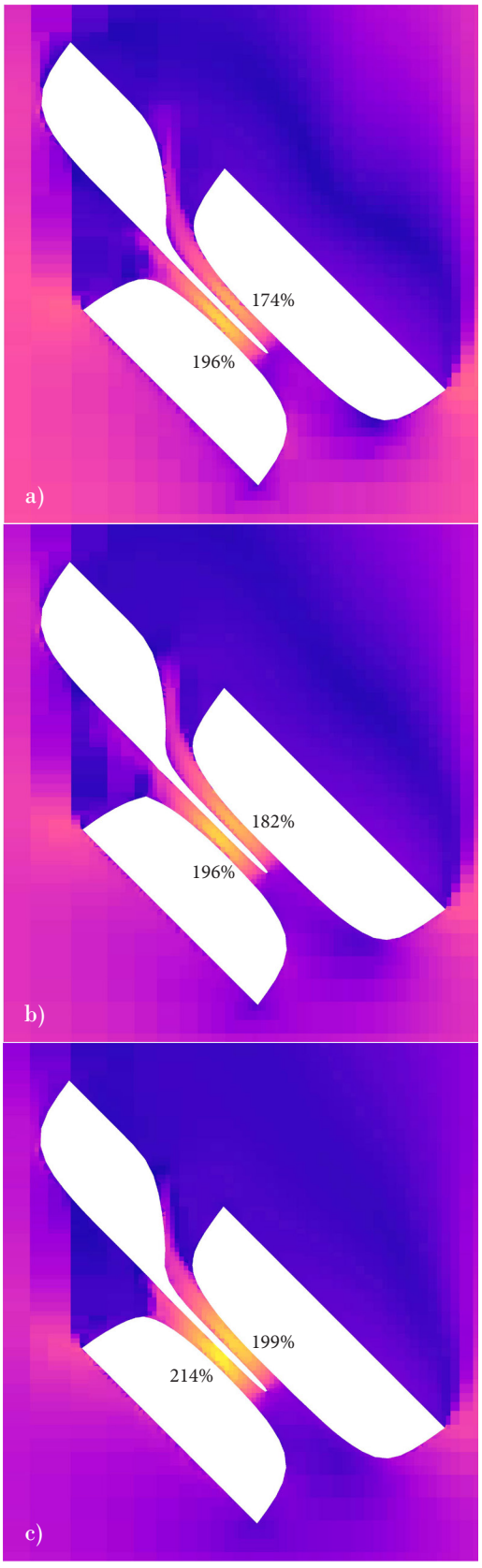

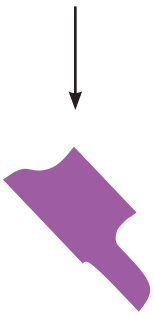

fig. 62
Simulation result for wind directionat 0°
in different heights-
a) 16.6m
b)12.25m
c)7.9m

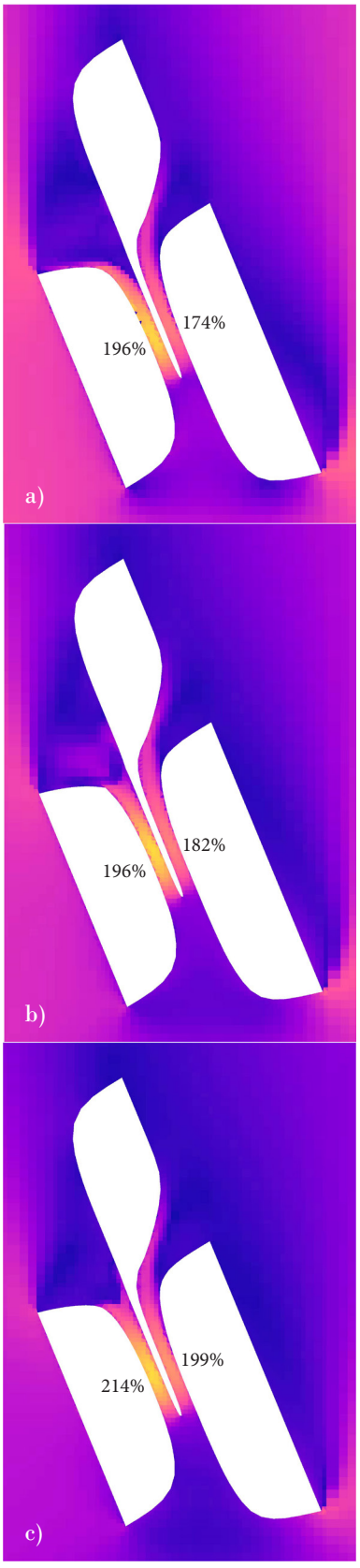

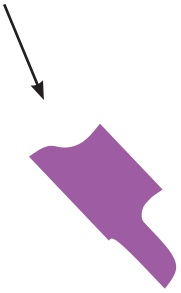

fig. 63
Simulation result for wind direction at 337.5°
at different heights-
a) 16.6m
b)12.25m
c)7.9m

fig. 64
Simulation result for wind direction at 315°
in different heights -
a) 16.6m
b)12.25
c)7.9m

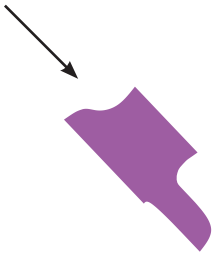

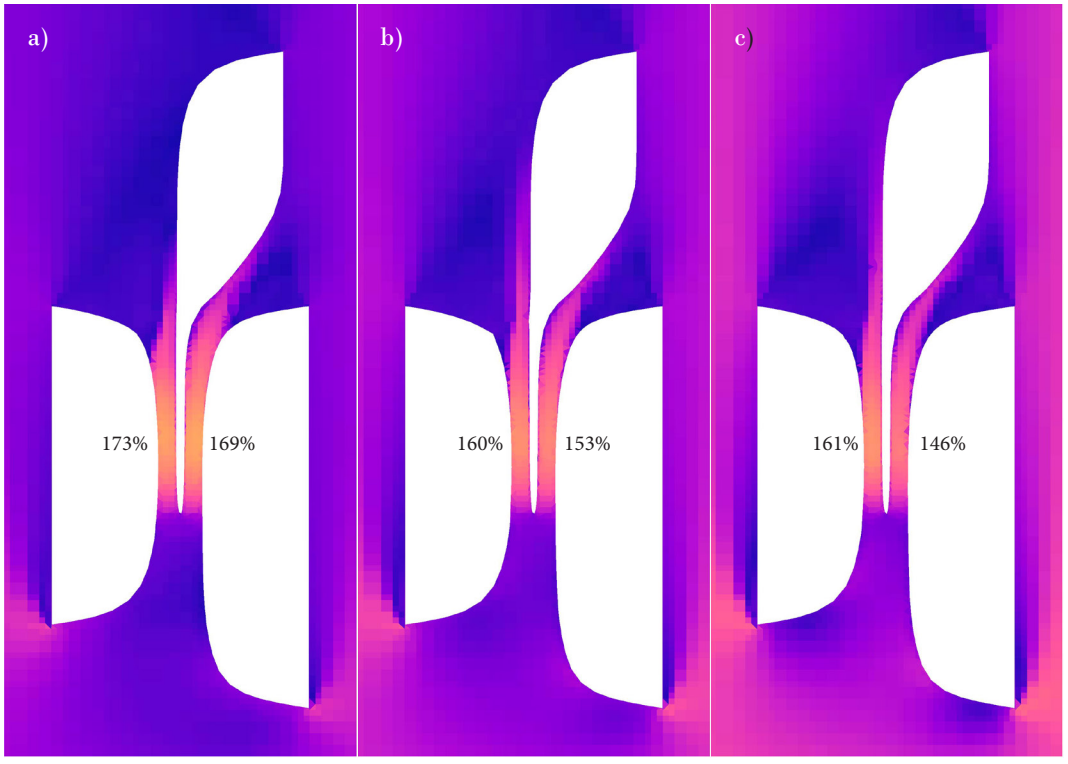

5. *Conclusion*

This project set to investigate the possibility of enhancing the windflow speed and possibility of wind energy collection in small scale by shaping a building volume on an example of low-rise residential building. It was shown that straightforward funneling shape as a spatial configuration is not neccesarily the optimal solution for this purpose. A variety of configurations was introduced which demonstrate how nuances in form of the building can lead to big differences in resulting performance.

The case study introduced a volume that can enhance the power output of a wind turbine while maintaining reasonable architectural layout. Despite not covering whole building energy demand it provides coverage for significant portion of annual energy loads and when paired with solar energy collection it creates a combination where wind turbines complement periods of lower solar energy collection.

The model was set into less densely built environment, nevertheless to validate performance results of the tested shape, performing larger scale CFD simulation that includes surrounding buildings would be necessary as other buildings would have influence on airflow around the studied volume. Larger CFD analysis would offer more insight not only in a configuration of one building volume but also in an interaction of multiple volumes and their mutual influence on airflow. Availability of computational resources pose an obstacle in this case as CFD analysis is very computationally expensive.

Futher research is needed to determine the range of effective applicability of wind enhancing spatial configuration in different urban contexts and wind patterns.

Bibliography:

Abohela, I., Hamza, N., & Dudek, S. (2013). Effect of roof shape, wind direction, building height and urban configuration on the energy yield and positioning of roof mounted wind turbines. Renewable Energy, 2013(50), 1106-1118. https://doi.org/https://doi.org/10.1016/j.renene.2012.08.068

Arteaga-López, E., Ángeles-Camacho, C., & Bañuelos-Ruedas, F. (2019). Advanced methodology for feasibility studies on building-mounted wind turbines installation in urban environment: Applying CFD analysis. Energy, 2019(167), 181-188. https://doi.org/https://doi.org/10.1016/j.energy.2018.10.191

Brown, G., & DeKay, M. (2001). Sun, wind & light : architectural design strategies. (2nd ed.). Wiley.

Cody, B. (2017). Form Follows Energy: Using natural forces to maximize performance (1st). Birkhäuser.
In focus: Renewable energy in Europe. (2020).

European Comission Website. Retrieved 2021-03-27, from https://ec.europa.eu/info/news/focus-renewable-energy-europe-2020-mar-18_en

KC, A., Whale, J., & Urmee, T. (2019). Urban wind conditions and small wind turbines in the built environment: A review. Renewable Energy, 2019(131), 268-283. https://doi.org/https://doi.org/10.1016/j.renene.2018.07.050

Kosky, P., Balmer, R., Keat, W., & Wise, G. (2021). Exploring Engineering: An Introduction to Engineering and Design (5th edition). Academic Press.

Letcher, T. (2017). Wind Energy Engineering: A Handbook for Onshore and Offshore Wind Turbines (1st). Academic Press.

Molnarova, K., Sklenicka, P., Stiborek, J., Svobodova, K., Salek, M., & Brabec, E. (2012). Visual preferences for wind turbines: Location, numbers and respondent characteristics. Applied Energy, (92), 269-278. https://doi.org/10.1016/j.apenergy.2011.11.001

Passive House requirements. (2015). Passive House Institute. Retrieved 2021-04-01, from https://passiv.de/en/02_informations/02_passive-house-requirements/02_passive-house-requirements.htm

Progress on energy efficiency in Europe. European Environment Agency. Retrieved 2021-04-01, from https://www.eea.europa.eu/data-and-maps/indicators/progress-on-energy-efficiency-in-europe-3/assessment

Smith, R., & Killa, S. (2007). Bahrain World Trade Center (BWTC): the first large-scale integration of wind turbines in a building. THE STRUCTURAL DESIGN OF TALL AND SPECIAL BUILDINGS, 16(4), 429-439. https://doi.org/https://doi.org/10.1002/tal.416

Stathopoulos, T., Alrawashdeh, H., Al-Quraan, A., Blocken, B., Dilimulati, A., Paraschivoiu, M., & Pilay, P. (2018). Urban wind energy: Some views on potential and challenges. Journal of Wind Engineering and Industrial Aerodynamics, (179), 146-157. https://doi.org/10.1016/j.jweia.2018.05.018

The Venturi effect. What it is and its application fields. Termotecnica Pericoli. Retrieved 2021-04-01, from https://www.pericoli.com/EN/news/119/The-Venturi-effect-What-it-is-and-its-application-fields.html

Tomlinson, R., Baker, W., Leung, L., Chien, S., & Zhu, Y. (2014). Case Study: Pearl River Tower, Guangzhou. CTBUH Journal, 2014(2), 11-17.

Tummala, A., Velamati, R., Sinha, D., Indraja, V., & Krishna, V. (2016). A review on small scale wind turbines. Renewable and Sustainable Energy Reviews, (56), 1351-1371. https://doi.org/10.1016/j.rser.2015.12.027

Wang, B., Cot, L., Adolphe, L., Geoffroy, S., & Sun, S. (2017). Cross indicator analysis between wind energy potential and urban morphology. Renewable Energy, (113), 989-1006. https://doi.org/10.1016/j.renene.2017.06.057

List of figures: